An Implementation Of Analytical and Numerical Methods For Moving-Boundary Physics

MATH 703 Course Project

Debabrata Auddya

Pure mathematics is, in its way, the poetry of logical ideas
Albert Einstein

Declaration

I certify that this is my own work and that all sources used from the internet, literature, or otherwise have been cited.

Debabrata Auddya
30th September 2021

Contents

List of Figures

1 Introduction

In applied science a wide class of problems involve moving boundary [1],[2] or phase changes that arise as a result of heat conduction with moving boundary conditions. One such classical example is the Stefan problem [3] which has been traditionally used as a basis of physical models in ice formation, evaporation, condensation etc. It gives a description of evolution of the boundary between two phases, and the heat equation is solved in those phases individually to obtain temperature distribution constrained with boundary and initial conditions (Page 151, [4]). In this project we aim to address couple of analytical methods which solve the Stefan problem and gives an intuitive understanding of the physics behind it. The methods discussed here are:

- The *similarity solution method* [5] which depend on certain groupings of the independent variables, rather than on each variable separately.
- *Perturbation method* are a class of analytical methods for determining approximate solutions of nonlinear equations for which exact solutions cannot be obtained [6]
- *Mixed variable analysis* also called multiple scale analysis in which the solutions depend simultaneously on multiple scales [7]
- *Polynomial analysis* which is used to approximate solutions to a PDE using substitutions [8]
- *Crank Nicholson finite difference scheme* to numerically evaluate characteristics of the moving boundary problem [9]

The following assumptions are used in most of the analytical methods

- All material properties are constant in the two phases
- Only solid-liquid interface problems are studied
- No viscous dissipation or turbulence is accounted for in the analysis.
- Internal thermodynamics or specifically internal heat generation is neglected.

2 Analytical Approach I: Similarity Solution

For the similarity solution three different situations (a) Solidification of a pure material in a superheated melt in which *three* different phases are considered and their dynamics solved using analytical techniques along with validating some results (b) Solidification of a pure material in an undercooled melt which considers *two* different phases. The interface evolution is first solved using standard methods and then plotted to visualise their patterns, and (c) A *single* phase is considered taking into account interface attachment kinetics in which the interface's velocity depends on the temperature difference.

2.1 Example I: Solidification of a pure material in a superheated melt

2.1.1 General Framework

For each of these scenarios, three distinct phases are considered and their energy balance equation (*Conversion of Fick's first law*, Page 339, [10]) in the reduced order form are written below:

$$\frac{\partial u_\nu}{\partial t} = \zeta_\nu \frac{\partial^2 u_\nu}{\partial x^2} \tag{1}$$

where $\nu = m, s, l$ refers to mold, solid, liquid respectively which means the three phases. In this equation $\zeta_\nu = k_\nu/\rho_\nu c_\nu$ represents the thermal diffusivity of the material or phase ν. The governing equation, boundary and initial conditions for the mold domain are:

$$\frac{\partial u_m}{\partial t} = \zeta_m \frac{\partial^2 u_m}{\partial x^2} \qquad -\infty < x \leq 0 \tag{2}$$

$$u_m = u_0 \qquad x \to \infty \tag{3}$$

$$u_m = u_{ms} \qquad x = 0 \tag{4}$$

$$k_m \frac{\partial u_m}{\partial x} = k_s \frac{\partial u_s}{\partial x} \qquad x = 0 \tag{5}$$

$$u_m = u_0 \qquad t = 0 \tag{6}$$

At the interface between mold and solid it can be seen that there are two boundary conditions $x = 0$. That is because the interface temperature between solid and mold is not known. Also the heat flux is continuous across the mold solid interface. The temperature distribution across the layers obeys $u \in C^1$ continuity condition. The governing equations for solid are:

$$\frac{\partial u_s}{\partial t} = \zeta_s \frac{\partial^2 u_s}{\partial x^2} \qquad 0 \leq x \leq x^*(t) \tag{7}$$

$$u_s = u_{ms} \qquad x = 0 \tag{8}$$

$$k_m \frac{\partial u_m}{\partial x} = k_s \frac{\partial u_s}{\partial x} \qquad x = 0 \tag{9}$$

$$u_s = u_f \qquad x = x^*(t) \tag{10}$$

$$\rho_s L_f \frac{dx^*}{dt} = k_s \frac{\partial u_s}{\partial x} - k_l \frac{\partial u_l}{\partial x} \qquad x = x^*(t) \tag{11}$$

The solid doesn't have an initial condition because the solidifying material is initially entirely liquid. At the solid liquid interface few boundary conditions need to applied as the *position* of the interface $x^*(t)$ is not known. The temperature of the interface is given as $T_f = u_f$. The second condition at the interface is known as the **Stefan condition**.

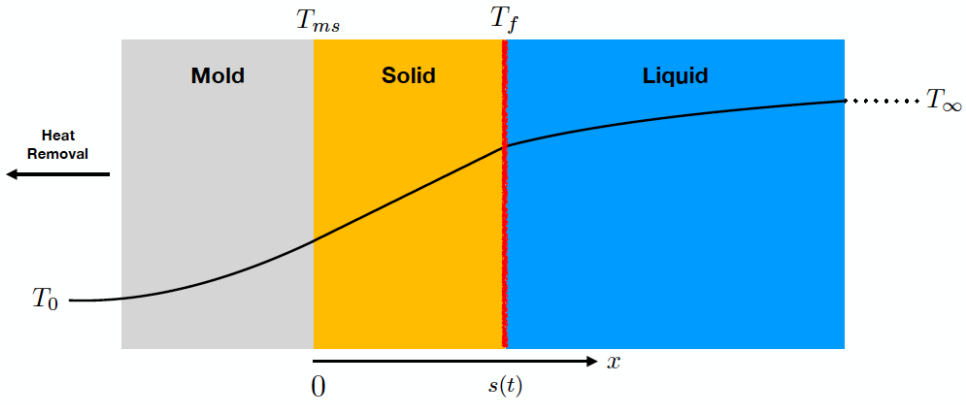

Figure 1: Superheated Solidification

Finally for the liquid phase the governing equations are:

$$\frac{\partial u_l}{\partial t} = \zeta_l \frac{\partial^2 u_l}{\partial x^2} \qquad x^* \leq x < \infty \tag{12}$$

$$u_l = u_\infty \qquad x \to \infty \tag{13}$$

$$u_l = u_f \qquad x = x^*(t) \tag{14}$$

$$\rho_s L_f \frac{dx^*}{dt} = k_s \frac{\partial u_s}{\partial x} - k_l \frac{\partial u_l}{\partial x} \qquad x = x^*(t) \tag{15}$$

$$u_l = u_\infty \qquad t = 0 \tag{16}$$

The analytical method [11],[12],[13],[14] used for all the three phases is presented after which boundary conditions are applied in all three phases to capture specific distributions. Similarity solution (*General similarity solution of the heat equation*, Page 4, [15]) method is used to analyse this PDE.

2.1.2 Similarity Solution

In the realm of partial differential equations there is an approach which identifies certain groupings of the independent variables rather than pure dependence on each of them separately which in turn converts it into an ordinary differential equation.While previous literature (*A similarity solution*, Page 3, [16]),(*The classical Stefan problem*, Page 3, [17]) used the analytical results to deal with solidification in binary alloys and fluid flow, a thorough derivation has been overlooked. The dilation transformation is introduced by:

$$\bar{X} = a^\alpha x, \qquad \bar{T} = a^\beta t, \qquad \bar{u}_\nu(\bar{X}, \bar{T}) = a^\gamma u_\nu(x,t) \tag{17}$$

$$x = a^{-\alpha}\bar{X}, \qquad t = a^{-\beta}\bar{T}, \qquad u_\nu(x,t) = a^{-\gamma}\bar{u}_\nu(\bar{X}, \bar{T}) \tag{18}$$

$$\frac{\partial \bar{u}_\nu}{\partial \bar{T}} = a^\gamma \frac{\partial u_\nu}{\partial \bar{T}} = a^\gamma \frac{\partial u_\nu}{\partial t}\frac{\partial t}{\partial \bar{T}} = a^{\gamma-\beta}\frac{\partial u_\nu}{\partial t} \tag{19}$$

$$\frac{\partial \bar{u}_\nu}{\partial \bar{X}} = a^\alpha \frac{\partial u_\nu}{\partial x}\frac{\partial x}{\partial \bar{X}} = a^{\gamma-\alpha}\frac{\partial u_\nu}{\partial x} \qquad \frac{\partial^2 \bar{u}_\nu}{\partial \bar{X}^2} = a^{\gamma-2\alpha}\frac{\partial^2 \bar{u}_\nu}{\partial x^2} \tag{20}$$

According to the similarity solution if $u(t,x)$ solves the original equation, then $\bar{U}(\bar{T}, \bar{X})$ satisfies the equation as well. Using this proposition:

$$(\bar{U}_\nu)_{\bar{T}} - \zeta_\nu (\bar{U}_\nu)_{\bar{X}\bar{X}} = a^{\gamma-\beta}(u_\nu)_t - \zeta_\nu a^{\gamma-2\alpha}(u_\nu)_{xx}$$

Comparing the left and right hand of side of the above equation it can be said that if $\bar{U}$ solves the equation as u, the common factor must be equal. This means that:

$$a^{\gamma-\beta} = a^{\gamma-2\alpha} \implies \beta = 2\alpha \tag{21}$$

thereby establishing a relationship between the two exponents and γ may be arbitrary. This is valid for all the three phases in consideration.

The next task is to find out the exponents p, q which satisfies the relation below. This is done to ensure that the following combinations are unchanged upon transformation.

$$\bar{X}\bar{T}^p = xt^p \qquad \bar{U}_\nu \bar{T}^q = u_\nu t^q \tag{22}$$

$$\bar{X}\bar{T}^p = a^{-\alpha}\bar{X}a^{-\beta p}\bar{T}^p \tag{23}$$

Using relation (21) it can be shown that

$$\alpha + 2\alpha p = 0 \implies p = -\frac{1}{2} \tag{24}$$

Thus it can be said that $xt^{-1/2}$ is the absolute invariant and also represents the characteristic variable. This idea can be extended to make it a dimensionless quantity by tweaking the denominator and rewriting the expression which we shall use later.

$$\frac{x}{\sqrt{\zeta_v t}} = \text{dimensionless} = \eta_\nu \tag{25}$$

An interesting fact to note here is that if we equate the above to 1, the resulting expression of x is also known as diffusion distance. Similarly, one can obtain an expression for q by using the second relation in (22)

$$\bar{U}_\nu \bar{T}^q = a^\gamma u_\nu (a^\beta t)^q = a^{\gamma+2\alpha q} u_\nu t^q \implies q = -\frac{\gamma}{2\alpha} \tag{26}$$

Since the exponent of a needs to be zero we could derive the following expression.

The parameters p, q are important because they help in setting up a relation between the actual solution and the new characteristic variable using the expression:

$$u_\nu(x,t) = t^{-q} g(xt^p) = t^{\frac{\gamma}{2\alpha}} g(xt^{-\frac{1}{2}}) = t^{\frac{\gamma}{2\alpha}} g(\xi) = t^{\frac{\gamma}{\beta}} g(\xi) \tag{27}$$

where ξ is the characteristic variable.

Substituting (27) into (1) we obtain the following.

$$(u_\nu)_t = \frac{\gamma}{\beta} t^{\frac{\gamma}{\beta}-1} g(xt^{-\frac{1}{2}}) + t^{\frac{\gamma}{\beta}} g'(xt^{-\frac{1}{2}})(-\frac{1}{2} xt^{-\frac{3}{2}}) = \frac{\gamma}{\beta} t^{\frac{\gamma}{\beta}-1} g(\xi) - \frac{1}{2} t^{\frac{\gamma}{\beta}-1} \xi g'(\xi) \tag{28}$$

$$(u_\nu)_{xx} = t^{\frac{\gamma}{\beta}-1} g''(\xi) \tag{29}$$

From the above it can be rewritten according to (1)

$$\begin{aligned}(u_\nu)_t - \zeta_\nu (u_\nu)_{xx} &= \frac{\gamma}{\beta} t^{\frac{\gamma}{\beta}-1} g(\xi) - \frac{1}{2} t^{\frac{\gamma}{\beta}-1} \xi g'(\xi) - \zeta_\nu t^{\frac{\gamma}{\beta}-1} g''(\xi) \\ &= t^{\frac{\gamma}{\beta}-1} (\frac{\gamma}{\beta} g(\xi) - \frac{1}{2} \xi g'(\xi) - \zeta_\nu g''(\xi)) = 0\end{aligned}$$

Since t cannot be equal to 0, we can consider the following expression below as zero and convert the original PDE into an ODE with the characteristic variable as its independent variable.

$$\zeta_\nu g''(\xi) + \frac{1}{2} \xi g'(\xi) - \frac{\gamma}{\beta} g(\xi) = 0 \tag{30}$$

To simplify one can use (4) to evaluate boundary values of g.

$$u_m(0,t) = u_{ms} \implies u_{ms} = g(0) t^{\frac{\gamma}{\beta}} \tag{31}$$

Since it is assumed that u_{ms} is a constant (which we shall find an analytical expression for eventually) meaning the exponent of t must be zero. Hence $\gamma = 0$ and (30) can be rewritten as

$$\zeta_\nu g''(\xi) + \frac{1}{2} \xi g'(\xi) = 0 \tag{32}$$

Using the integrating factor method for linear homogeneous ODEs the following is derived for $g(\xi)$

$$g'(\xi) = C_1 e^{-\int \frac{\xi}{2\zeta_\nu} d\xi} = C_1 e^{-\frac{\xi^2}{4\zeta_\nu}} \tag{33}$$

$$g(\xi) = C_0 + C_1 e^{-\int_0^\xi \frac{\chi^2}{4\zeta_\nu} d\chi} = C_0 + C_2 \text{erf}(\frac{\xi}{\sqrt{4\zeta_\nu}}) = C_0 + C_2 \text{erf}(\frac{x}{2\sqrt{\zeta_\nu t}}) \tag{34}$$

2.1.3 Temperature distribution of mold

As the characteristic equation differs only in terms of the thermal diffusivity and the boundary conditions it can be said that for all three phases the equation has a general form:

$$u_\nu = A_\nu + B_\nu \text{erf}(\frac{x}{2\sqrt{\zeta_\nu t}}) \tag{35}$$

Since the equation (34) obtains a general solution for the different phases one can utilise this for obtaining temperature distribution in the mold phase to begin with $u_m(x,t)$.

$$u_m(0,t) = C_0 + C_2\text{erf}(0) = u_{ms} \implies C_0 = u_{ms} \tag{36}$$

$$u_m(-\infty,t) = u_{ms} + C_2\text{erf}(-\infty) = u_0 \implies C_2 = u_{ms} - u_0 \tag{37}$$

The above relation is established using the identity

$$\frac{2}{\sqrt{\pi}}\int_0^\infty e^{-t^2}dt = 1 \tag{38}$$

Thus, for the mold phase the general solution can be written as

$$\boxed{u_m(x,t) = u_{ms} + (u_{ms} - u_0)\text{erf}(\frac{x}{2\sqrt{\zeta_m t}}) \qquad -\infty < x \leq 0} \tag{39}$$

2.1.4 Temperature distribution of solid

At this point, though we have stated that u_{ms} is a constant, it is unknown and needs to be calculated. The second way by which u_{ms} can be evaluated, since most boundary conditions of the mold phased are used, is by considering the adjacent solid phase. The general solution for this phase can be written in the form of (35).

$$u_s = A_s + B_s\text{erf}(\frac{x}{2\sqrt{\zeta_s t}}) \tag{40}$$

Applying (8) and (10) the general expression is rewritten as

$$u_s(0,t) = A_s + B_s\text{erf}(0) = u_{ms} \implies A_s = u_{ms} \tag{41}$$

$$u_s(x^*(t),t) = u_f = u_{ms} + B_s\text{erf}(\frac{x^*(t)}{2\sqrt{\zeta_s t}}) \tag{42}$$

Since the interface temperatures u_f and u_{ms} are assumed to be constant, therefore the error function must be a constant as well. Thus it implies, $x^*(t)$ is proportional to $2\sqrt{\zeta_s t}$.

$$x^*(t) = 2\phi\sqrt{\zeta_s t} \tag{43}$$

where ϕ is a constant and will be determined eventually. However the above gives a general solution for the *boundary evolution* of the solid and liquid phases.

Now we can calculate B_s from (42) using the above

$$u_f = u_{ms} + B_s\text{erf}(\phi) \implies B_s = \frac{u_f - u_{ms}}{\text{erf}(\phi)} \tag{44}$$

$$\therefore \boxed{u_s = u_{ms} + \frac{u_f - u_{ms}}{\text{erf}(\phi)}\text{erf}(\frac{x}{2\sqrt{\zeta_s t}}) \qquad 0 \leq x \leq x^*(t)} \tag{45}$$

2.1.5 Temperature of solid-mold interface

Since we have analytical expression for all components of the temperature distribution equation in the solid (45) and mold (39) phase, the interface temperature u_{ms} can be evaluated using flux condition of (9)

$$k_m \frac{\partial}{\partial x}(u_{ms} + (u_{ms} - u_0)\text{erf}(\frac{x}{2\sqrt{\zeta_m t}})) = k_s \frac{\partial}{\partial x}(u_{ms} + \frac{u_f - u_{ms}}{\text{erf}(\phi)}\text{erf}(\frac{x}{2\sqrt{\zeta_s t}})) \tag{46}$$

The expression $\sqrt{k_\nu \rho_\nu c_{p\nu}} = \Phi_\nu$ is known as effusivity (*Results and Discussion*, Page 4, [18]) of the material and will be used here. Derivative of the error function can be written in the form.

$$\frac{\partial}{\partial x}\text{erf}(u) = \frac{2}{\sqrt{\pi}} e^{-u^2} \frac{\partial u}{\partial x} \tag{47}$$

Rearranging terms we have:

$$\Phi_m(u_{ms} - u_0) = \frac{\Phi_s}{\text{erf}(\phi)}(u_f - u_{ms})$$

$$(\text{erf}(\phi)\Phi_m + \Phi_s)u_{ms} = \text{erf}(\phi)\Phi_m u_0 + \Phi_s u_f$$

The mold-solid interface temperature is thus,

$$\boxed{u_{ms} = \frac{\text{erf}(\phi)\Phi_m u_0 + \Phi_s u_f}{\text{erf}(\phi)\Phi_m + \Phi_s}} \tag{48}$$

2.1.6 Temperature distribution of liquid

The solution for temperature in the liquid phase is obtained by replacing time derivative of (43) into (15). We begin with the general solution for the liquid phase

$$u_l = A_l + B_l \text{erf}(\frac{x}{2\sqrt{\zeta_l t}}) \tag{49}$$

Using (13) and (16) into (49) one obtains

$$u_l = A_l + B_l \text{erf}(+\infty) = u_\infty \implies A_l + B_l = u_\infty \tag{50}$$

Also using (14) into (49) another relation is observed

$$u_f = A_l + B_l \text{erf}(\frac{x^*(t)}{2\sqrt{\zeta_l t}}) \tag{51}$$

Replacing (43) the following is obtained

$$u_f = A_l + B_l \text{erf}(\phi\sqrt{\frac{\zeta_s}{\zeta_l}}) \tag{52}$$

Since we have two equations, (50) and (52) with two unknowns it is easy to obtain expressions for A_l and B_l

$$A_l = \frac{u_f - u_\infty \text{erf}(\phi\sqrt{\frac{\zeta_s}{\zeta_l}})}{\text{erfc}(\phi\sqrt{\frac{\zeta_s}{\zeta_l}})} \qquad B_l = \frac{u_\infty - u_f}{\text{erfc}(\phi\sqrt{\frac{\zeta_s}{\zeta_l}})} \tag{53}$$

where erfc $= 1 -$ erf. Now plugging these into (49) we obtain

$$u_l = \frac{u_f - u_\infty \text{erf}(\phi\sqrt{\frac{\zeta_s}{\zeta_l}})}{\text{erfc}(\phi\sqrt{\frac{\zeta_s}{\zeta_l}})} + \frac{u_\infty - u_f}{\text{erfc}(\phi\sqrt{\frac{\zeta_s}{\zeta_l}})}\text{erf}(\frac{x}{2\sqrt{\zeta_l t}})$$

A cleaner version of the above is given as:

$$\boxed{u_l = u_\infty - \frac{u_\infty - u_f}{\text{erfc}(\phi\sqrt{\frac{\zeta_s}{\zeta_l}})}\text{erfc}(\frac{x}{2\sqrt{\zeta_l t}}) \qquad x^*(t) \leq x < \infty} \tag{54}$$

2.1.7 Determination of parameter ϕ

In order to find the parameter ϕ the Stefan condition (15) is utilised. Plugging in the values from (45),(48) and (54) the following relation is obtained.

$$\rho_s L_f \phi \sqrt{\frac{\zeta_s}{t}} = k_s\left(\frac{u_f - u_{ms}}{\text{erf}(\phi)} \frac{1}{\sqrt{\pi \zeta_s t}} \exp\left(-\frac{x}{2\sqrt{\zeta_s t}}\right)^2\right) - k_l\left(\frac{u_\infty - u_f}{\text{erfc}(\phi\sqrt{\frac{\zeta_s}{\zeta_l}})} \frac{1}{\sqrt{\pi \zeta_l t}} \exp\left(-\frac{x}{2\sqrt{\zeta_l t}}\right)^2\right) \quad (55)$$

Rearranging the above we get the following *transcendental equation* for ϕ, which is usually solved using graphical methods.

$$\boxed{\left(\phi \exp(\phi^2) - \frac{c_{ps}(u_\infty - u_f)}{L_f\sqrt{\pi}} \frac{\exp([1-\zeta_s/\zeta_l]\phi^2)}{\text{erfc}(\phi\sqrt{\zeta_s/\zeta_l})} \sqrt{\frac{\Phi_l}{\Phi_s}}\right) \times \left(\text{erf}(\phi) + \sqrt{\frac{\Phi_s}{\Phi_m}}\right) = \frac{c_{ps}(u_f - u_0)}{L_f\sqrt{\pi}} = \frac{\text{Ste}}{\sqrt{\pi}}} \quad (56)$$

The Stefan number is given by the expression

$$\text{Ste} = \frac{c_{ps}(u_f - u_0)}{L_f} \quad (57)$$

Equation (56) gives only a constant which determines the factor of proportionality for evolution of the interface between the solid and liquid phases.

This equation can be solved graphically by assuming couple of values for the parameters given and determining the proportionality constant

2.1.8 Graphical estimation of ϕ

To determine ϕ some sample parameters [4] are used which are as follows along with $L_f = 3.98 \times 10^5 J/kg$:

Material	Temperature C	Thermal conductivity $Wm^{-1}K^{-1}$	Specific Heat $Jkg^{-1}K^{-1}$	Density kgm^{-3}
Mold	25	100	1700	2200
Solid	660	211	1190	2555
Liquid	700	91	1090	2368

Inserting the above values in (56), we obtain the following expression for ϕ

$$(\phi \exp\phi^2 - 0.041\frac{\exp(-0.968\phi^2)}{\text{erc}(1.403\phi)}) \times (\text{erf}(\phi) + 1.304) = f(\phi) = \frac{\text{Ste}}{\sqrt{\pi}} = 1.071 \quad (58)$$

In order to find out the roots of the above equation we need to find out the residual and set it to zero. Accordingly, we have the expression as:

$$g(\phi) = f(\phi) - \frac{\text{Ste}}{\sqrt{\pi}} = 0 \quad (59)$$

The plot below indicates that the residual function intersects the zero ordinate when the value of ϕ is about 0.52. Hence this can be replaced back into the interface evolution equation and into (48),(54),(45),(39) from which we obtain the following expressions of temperature distributions for this example case

$$x^*(t) = 8.7 \times 10^{-3}\sqrt{t} \quad (60)$$

$$u_m = 474 + 443\text{erf}(97.05\frac{x}{\sqrt{t}}) \quad (61)$$

$$u_s = 474 + 346\text{erf}(61.9\frac{x}{\sqrt{t}}) \quad (62)$$

$$u_l = 698 - 135\text{erfc}(85.3\frac{x}{\sqrt{t}}) \quad (63)$$

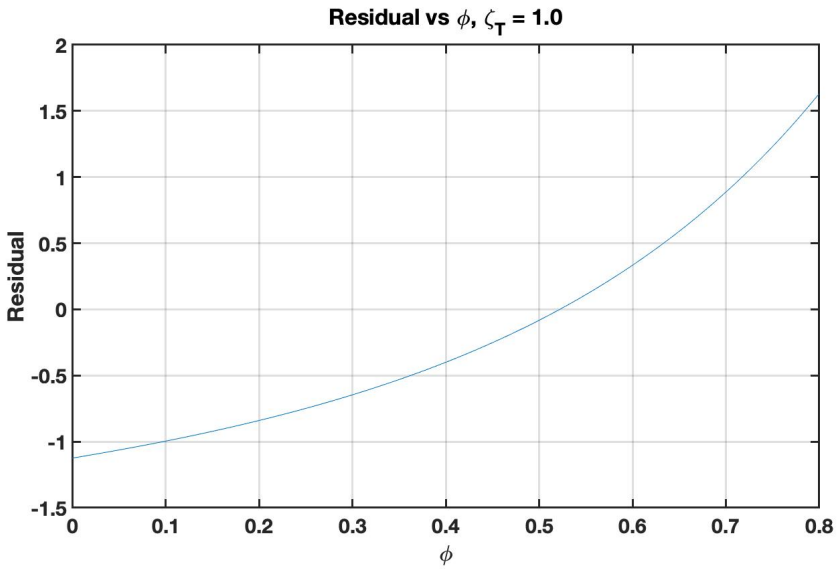

Figure 2: Determination of ϕ using graphical method

In conclusion to the first task we calculated the temperature distribution in three phases as well as the interface temperatures and their evolution in a superheated melt.

2.2 Example II: Solidification of a pure material in an undercooled melt

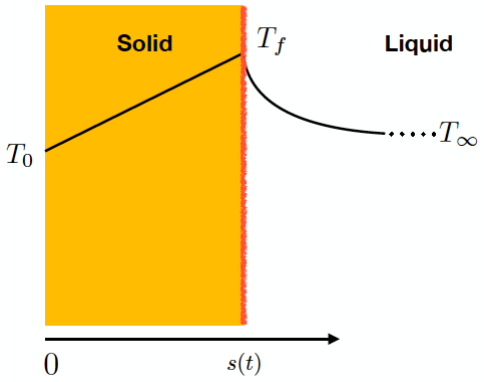

Figure 3: Supercooled Solidification

A one dimensional solidification of a pure material with a planar front growing into an undercooled melt (Appendix II, Page 122, [19]) is considered (Fig 2). Since the interface has a higher temperature than both the semi infinite end (liquid) as well as the solid, heat starts flowing out of the interface in both solid and liquid. The goal here is to track the evolution of the interface as well as determining the temperature distributions in the two phases. In addition to this, **interface attachment kinetics** (Section VII: *Towards predictive capability of rapid solidification in commercial alloys*, Page 10, [20]) is introduced and analytical solutions are derived for a case involving freezing consisting of an isothermal solid and an undercooled melt.

2.2.1 General framework and field distributions

Referring to Fig 3, it is seen that the semi infinite melt begins at $u_f > u_\infty$. Also when time $t = 0$, the left hand side of the boundary cools to $u_s = u_0, u_0 < u_f$. This is a classic case of bidirectional heat flow from the interface to the solid and liquid phases. The governing equations for the two phases are as follows:

$$\frac{\partial u_s}{\partial t} = \zeta_s \frac{\partial^2 u_s}{\partial x^2} \qquad 0 \le x \le x^*(t) \tag{64}$$

$$\frac{\partial u_l}{\partial t} = \zeta_l \frac{\partial^2 u_l}{\partial x^2} \qquad x^*(t) \le x < \infty \tag{65}$$

$$u_s = u_0 \qquad x = 0 \tag{66}$$

$$u_l = u_\infty \qquad x \to \infty \tag{67}$$

$$u_s = u_l = u_f \qquad x = x^*(t) \tag{68}$$

$$k_s \frac{\partial u_s}{\partial x} - k_l \frac{\partial u_l}{\partial x} = \rho L_f \frac{dx^*}{dt} \qquad x = x^*(t) \tag{69}$$

The above problem can be solved in a similar manner using the similarity solution. Since the governing equation is the same as in the previous equation in which the temperature distribution had a general solution. Hence rewriting (35)

$$u_\nu = A_\nu + B_\nu \text{erf}(\frac{x}{2\sqrt{\zeta_\nu t}})$$

For the solid phase, replacing (35) with (66) we obtain

$$A_s = u_0$$

Since the interface temperature is a constant in this case we can say that the argument in erf is a constant. Thus the modified equation is:

$$u_f = u_0 + B_s \text{erf}(\phi)$$

where ϕ is the proportionality constant as seen in the previous section. Thus the final version of the temperature distribution in the solid phase based on the boundary conditions are:

$$u_s = u_0 + \frac{u_f - u_0}{\text{erf}(\phi)} \text{erf}(\frac{x}{2\sqrt{\zeta_s t}}) \tag{70}$$

For the liquid region, the analysis is performed in a similar way in which we obtain the values of the general solution parameters A_l and B_l as

$$A_l = u_\infty \quad B_l = \frac{u_f - u_\infty}{\text{erfc}(\phi\sqrt{\zeta_s/\zeta_l})} \text{erfc}(\frac{x}{2\sqrt{\zeta_l t}})$$

Thus, temperature distribution in the liquid region is given by:

$$u_l = u_\infty + \frac{u_f - u_\infty}{\text{erfc}(\phi\sqrt{\zeta_s/\zeta_l})} \text{erfc}(\frac{x}{2\sqrt{\zeta_l t}}) \tag{71}$$

2.2.2 Analytical solution of ϕ

Since we have the interface evolution of the form $x^*(t) = 2\phi\sqrt{\zeta_s t}$ the proportionality constant can be found out using the Stefan condition (69). Replacing u_s and u_l in the equation we can obtain

$$k_s \frac{\partial}{\partial x}(u_0 + \frac{u_f - u_0}{\text{erf}(\phi)} \text{erf}(\frac{x}{2\sqrt{\zeta_s t}})) - k_l \frac{\partial}{\partial x}(u_\infty + \frac{u_f - u_\infty}{\text{erfc}(\phi\sqrt{\zeta_s/\zeta_l})} \text{erfc}(\frac{x}{2\sqrt{\zeta_l t}})) = \rho_s L_f \phi \sqrt{\frac{\zeta_s}{t}}$$

$$\implies k_s \frac{u_f - u_0}{\text{erf}(\phi)} (\frac{1}{\sqrt{\pi\zeta_s t}} \exp(-\frac{x}{2\sqrt{\zeta_s t}})^2) + k_l \frac{u_f - u_\infty}{\text{erfc}(\phi\sqrt{\zeta_s/\zeta_l})} (\frac{1}{\sqrt{\pi\zeta_l t}} \exp(-\frac{x}{2\sqrt{\zeta_l t}})^2) = \rho_s L_f \phi \sqrt{\frac{\zeta_s}{t}}$$

Replace $x = x^*(t), k_\nu = \zeta_\nu \rho_\nu c_\nu, \rho_s = \rho_l = \rho, \zeta_s/\zeta_l = \zeta_T$ in the above equations we obtain

$$c_{ps}\sqrt{\frac{\zeta_T}{\pi}}\frac{u_f - u_0}{u_f - u_\infty}\frac{e^{-\phi^2}}{\text{erf}(\phi)} + c_{pl}\sqrt{\frac{1}{\pi}}\frac{e^{-\phi^2}}{\text{erfc}(\phi\sqrt{\zeta_T})} = L_f\phi\frac{\sqrt{\zeta_T}}{u_f - u_\infty}$$

Since the Stefan number is given as, $\text{Ste} = \frac{u_f - u_\infty}{L_f/c_{ps}}$ and $\beta = \frac{c_{ps}(u_f - u_0)}{c_{pl}(u_f - u_\infty)}$ we can use these replacements in the above equation and obtain the following form

$$\boxed{\text{Ste} = \frac{c_{pl}/c_{ps}}{\beta/[\sqrt{\pi}\phi\text{exp}(\phi^2)\text{erf}(\phi)] + 1/[\sqrt{\pi\zeta_T}\phi\text{exp}(\zeta_T\phi^2)\text{erfc}(\sqrt{\zeta_T}\phi)]}} \tag{72}$$

2.2.3 Graphical solution of ϕ

This is a transcendental equation and the value of ϕ can only be obtained by graphical methods.For simplicity Some parameters in (72) are varied, such as $\beta = 0.0, 0.2, 0.4, 0.6, 0.8$ and $\zeta_T = 1.0, 1.2, 1.4$, after which a graph of Ste vs ϕ is plotted. Additionally for this example the specific heats for the solid and liquid phase is assumed to same $c_{ps} = c_{pl}$ The value of ϕ can be

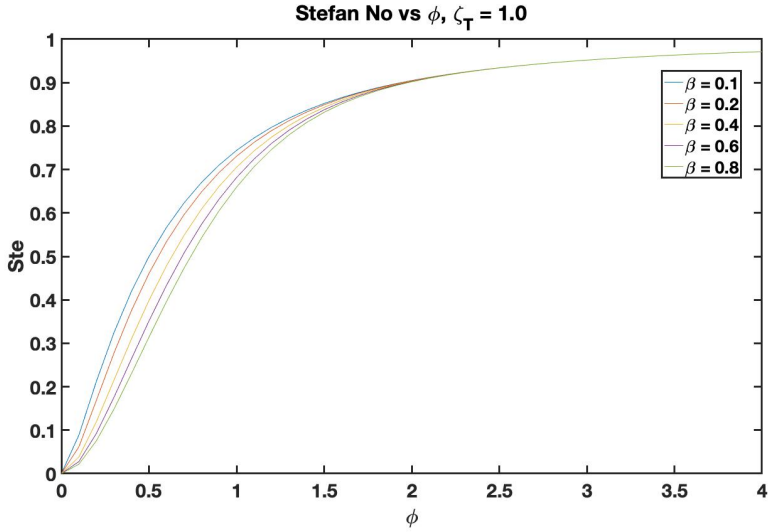

Figure 4: Stefan Number vs ϕ, $\zeta_T = 1.0$

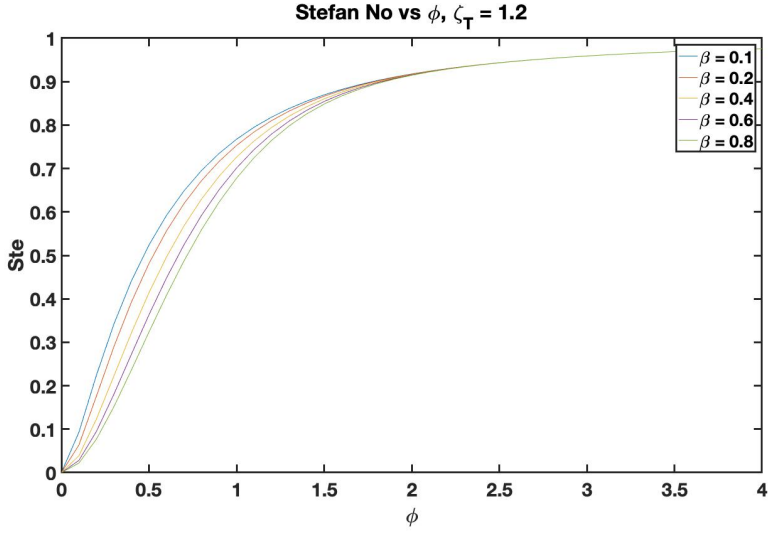

Figure 5: Stefan Number vs ϕ, $\zeta_T = 1.2$

obtained when the Stefan number is known. For instance (Section III: *One dimensional freezing of ice with constant heat flux in the water layer*, Page 24, [21]) mentioned that ice has a Stefan number of about Ste = 0.46. From the graph above we can see that this corresponds to a value of ϕ about 0.65.

2.2.4 Some Contradictions

Based on the graphical methods, [4] mentioned on Page 174 "At large undercooling, the interface velocity will be quite high (notice that $\phi \to \infty$ as Ste $\to 1$)". The above statement however is not **fully correct**. Using the given expression (72) the following plots reveal that within a fixed range of β and ζ_T, Ste is possible to be calculated for only a limited window of ϕ.

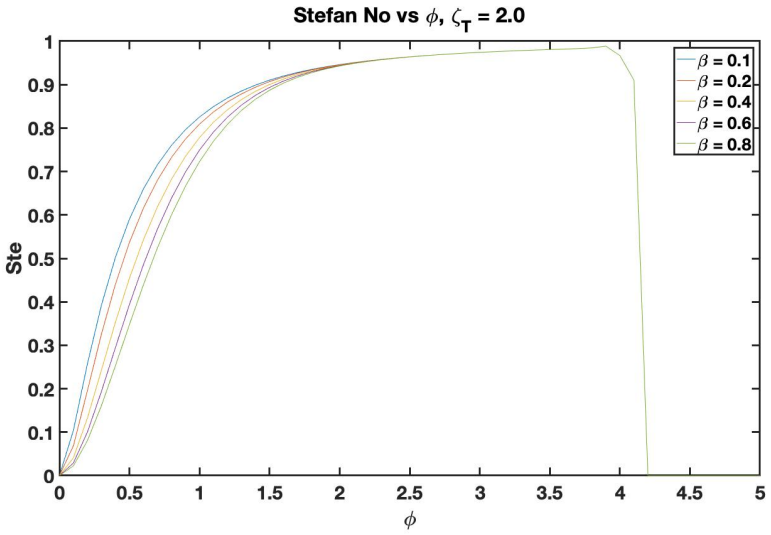

Figure 6: Stefan Number vs ϕ, $\zeta_T = 2.0$

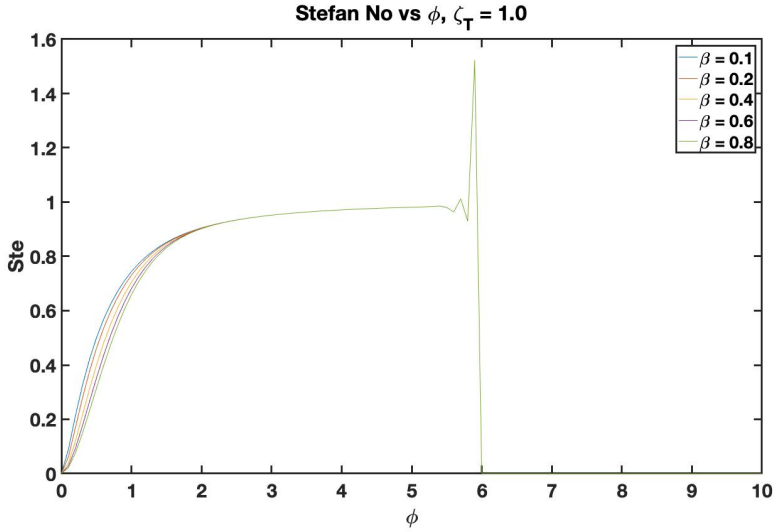

Figure 7: Stefan Number vs ϕ, $\zeta_T = 1.0$

2.2.5 Temperature distribution profiles

Based on the above value of ϕ obtained in the previous section we can plot the temperature profile as hypothesized in Fig 3

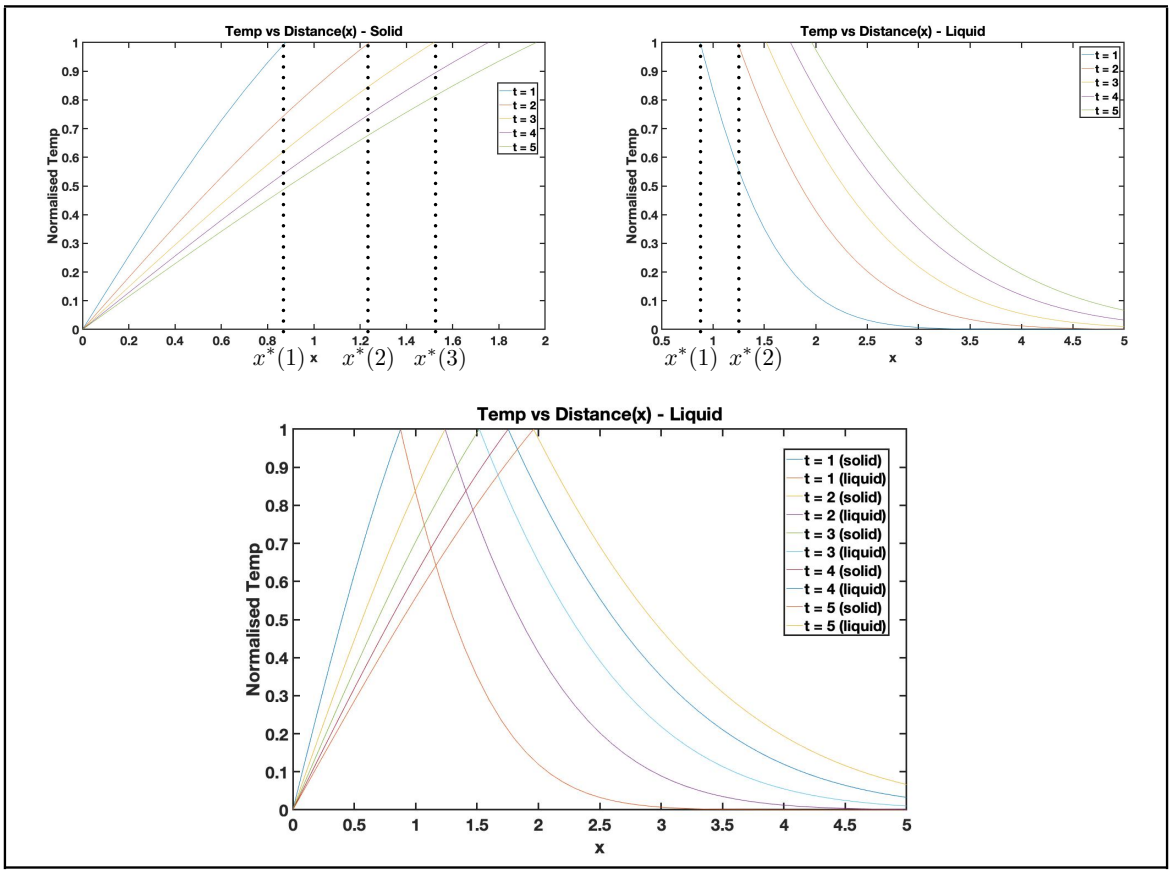

Figure 8: Temperature Distribution in Undercooled melt

The figure above explains that as the value of t increases, the interface,denoted by $x^*(t)$, proceeds towards right as indicated in the figure above. The top left figure describes the evolution of temperature in solid region with the corresponding evolution interface markers, followed by the top right which depicts temperature in the liquid regime for different intervals of time. The bottom figure combines the two and replicates Fig 3 for different intervals.

2.3 Example III: Interface attachment kinetics

Growth kinetics can be divided into diffusion kinetics and interface attachment kinetics (*Attachment Kinetics on Ideal Facet Surfaces*, Page 89, [22]), (*Kinetic Effects in PVA*, Page 9, [23]). While the former can be used for slow interface velocities, the later must be included for high speeds. The *Stefan number* is a useful metric to determine the kinetics of such problems. We demonstrated in the previous two sections that the Ste ≤ 1. In this example we see that Ste > 1 and extend the case of undercooling in which the solid is considered isothermal and the velocity is considered proportional to undercooling.

2.3.1 General Framework

$$\frac{\partial u_l}{\partial t} = \zeta_l \frac{\partial^2 u_l}{\partial x^2} \qquad x^* \leq x < \infty \tag{73}$$

$$u(x^*, t) = u^* = u_f - \frac{1}{\mu_k}\frac{dx^*}{dt} \qquad x = x^*(t) \tag{74}$$

$$\rho L_f \frac{dx^*}{dt} = -k_l \frac{\partial u_l}{\partial x} \qquad x = x^*(t) \tag{75}$$

$$u_l = u_\infty, \qquad x \to \infty, t = 0 \tag{76}$$

$$x^*(0) = x^* = 0 \qquad t = 0 \tag{77}$$

In this analysis the interface velocity,v^* is related to its undercooling Δu given by:

$$v^* = \frac{dx^*}{dt} = \mu_k \Delta u = \mu_k (u_f - u^*) \tag{78}$$

A technique to solve this problem is by employing a dimensionless system of equations which is given by:

$$\theta_l = \frac{u_l - u_\infty}{u_f - u_\infty} = (u_l - u_\infty)/\Delta u; \quad \xi = \frac{x}{L}; \quad \xi^*(\tau) = \frac{x^*(t)}{L}; \quad \tau = \frac{\zeta_l t}{L^2} \tag{79}$$

The modified set of dimensionless equations now transform to

$$\frac{\partial \theta_l}{\partial \tau} = \frac{\partial^2 \theta_l}{\partial \xi^2} \qquad \xi^*(\tau) \leq \xi < \infty \tag{80}$$

$$\theta_l = \theta^* \qquad \xi = \xi^*(\tau) \tag{81}$$

$$\frac{1}{\text{Ste}}\frac{d\xi^*}{d\tau} = -\frac{\partial \theta_l}{\partial \xi} \qquad \xi = \xi^*(\tau) \tag{82}$$

$$\theta_l = 0 \qquad \xi \to \infty, \tau = 0 \tag{83}$$

$$\xi^* = 0 \qquad \tau = 0 \tag{84}$$

The interface velocity (78) can be rescaled according to the following individual transformations (79) leading to

$$\begin{aligned}\frac{\zeta_l}{\mu_k L}\frac{d\zeta^*}{d\tau} &= (u_f - u_\infty - u^* + u_\infty)\frac{u_f - u_\infty}{u_f - u_\infty} \\ &= (1 - \frac{u^* - u_\infty}{u_f - u_\infty})(u_f - u_\infty) \\ &= (1 - \theta^*)\Delta u\end{aligned}$$

Thus the length scale which corresponds to a *competition* between diffusion and attachment kinetics is given by this expression

$$\frac{\zeta_l}{\mu_k L \Delta u}\frac{d\zeta^*}{d\tau} = 1 - \theta^* \qquad L = \frac{\zeta_l}{\mu_k \Delta u} \tag{85}$$

Another constraint which we have is that the velocity, v^* must be a constant since first there is no additional driving force that will cause it to change with time and secondly θ^* is also a constant.

2.3.2 Change of reference frame

At this point it is convenient to attach the frame of reference to the interface so that the temperature field is steady in this frame owing to (78). The transformation will only be along the x direction which can be modified as:

$$\chi = \xi - v^*\tau \tag{86}$$

Using this transformation, $\frac{\partial \chi}{\partial \tau} = -v^*$, $\frac{\partial^2 \chi}{\partial \zeta^2} = 1$ which is the modified diffusion equation becomes

$$(-v^*)\frac{\partial \theta_l}{\partial \chi} = \frac{\partial^2 \theta_l}{\partial \chi^2} \tag{87}$$

The revised boundary conditions for the changed reference variable are

$$\xi = \xi^* \implies \chi = 0; \quad \xi \to \infty \implies \chi \to \infty$$

At this point we have two boundary conditions and an ODE in which θ_l depends only on χ. Thus (87) can also be written in terms of an ODE without loss of generality. To solve this we use the face that v^* is a constant

$$\frac{\partial^2 \theta_l}{\partial \chi^2} + \frac{\partial v^* \theta_l}{\partial \chi} = 0$$
$$\implies \frac{\partial}{\partial \chi}\left(\frac{\partial \theta_l}{\partial \chi} + v^*\theta_l\right) = 0 \implies \frac{\partial \theta_l}{\partial \chi} + v^*\theta_l = 0$$

Given boundary conditions $\xi = 0 \implies \theta_l = \theta^*$

$$\boxed{\theta_l = \theta^* e^{-v^*\chi}} \tag{88}$$

Replacing (88) into the Stefan condition (82), the following values are obtained for θ^* and v^*

$$\frac{1}{\text{Ste}}\frac{d\xi^*}{dt}\frac{dt}{d\tau} = \theta^* v^* \implies \boxed{\theta^* = \frac{1}{\text{Ste}}}$$

Using (85) and plugging in the value of θ^* from above we have

$$v^* = 1 - \theta^* \implies \boxed{v^* = 1 - \frac{1}{\text{Ste}}} \tag{89}$$

Couple of observations follow from the above two results, most importantly, the Stefan number cannot be less than one. If it does, θ^* will be greater than one which is not possible since it is normalised. Secondly v^* cannot be negative as it will be an unphysical result in terms of interface movement.

2.3.3 Graphical Interpretation

We demonstrate a couple of important conclusions from the temperature variation away from the interface using the following plot.

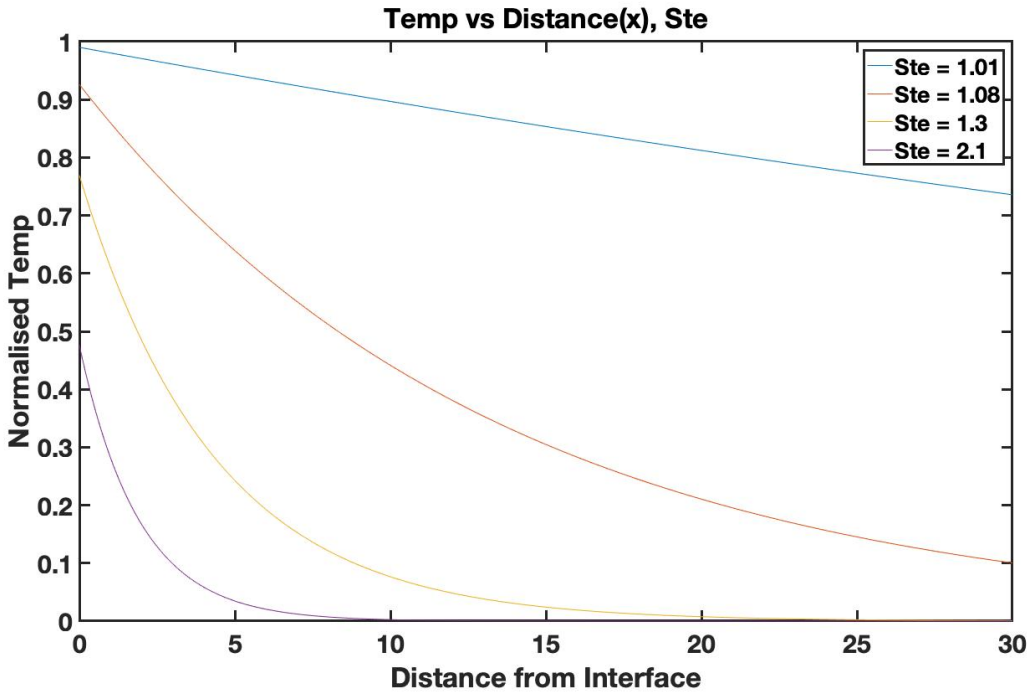

Figure 9: Temperature distribution in an advancing planar front

The Stefan number is varied for four different cases and the results show that

- When the Stefan number is close to 1 the interface temperature is higher and decreases fairly linearly
- When the undercooling is higher, meaning higher Stefan number, the decrease in temperature across the planar front is rapid
- The rate at which temperature drops *increases* as the Stefan number rises for lower starting values of interface temperature at $x = 0$
- The interface temperature is most sensitive when Stefan number is between $1 - 2$

3 Analytical Approach II: Perturbation Method

Perturbation theory is a branch of mathematics that deals with obtaining an approximate solution to a problem by starting with the exact solution of a related, simpler problem. The technique includes an intermediate phase that divides the problem into solvable and perturbative halves. The answer is given as a power series of a tiny parameter ϵ which represents the perturbation. The known solution to the solvable problem is the first phrase. At higher powers of ϵ, successive terms in the series normally become smaller [24],[25]. By truncating the series and maintaining only the first few terms, the solution to the known problem, and the first few orders of perturbation correction, an approximate perturbation solution is obtained. [6].

3.1 Perturbation solution to the Stefan problem

Perturbation theory produces a formal power series known as a perturbation series in some "small" parameter that quantifies the divergence from the precisely solved problem. The solution of the absolutely solvable problem is the first term in this power series, while subsequent terms describe the divergence in the answer caused by the deviation from the initial problem.

3.1.1 Introduction

The mathematical class of problems which involve a moving boundary are called Stefan problems which we have seen earlier in the analysis using similarity solution. For this implementation we root back to its original usage in freezing problem (also called *solidification*) of a saturated liquid.

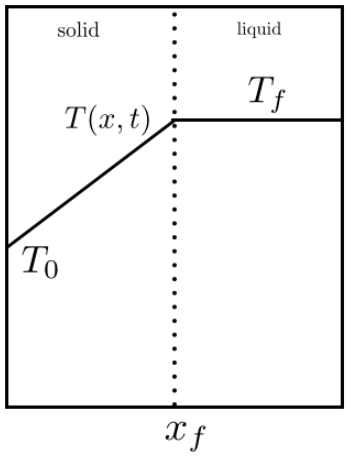

Figure 10: One dimensional freezing of a given region

In this problem the liquid considered is at a freezing temperature T_f after which the temperature is dropped to subfreezing value $T_0 < T_f$. Lowering of surface temperature at a location denoted by x_f which for this problem is the solidification *interface* causes the liquid to freeze and proceed with an advancing front. Having said this is a highly idealised model (useful for analysis) and incorporates the following assumptions:

- Solid and Liquid are both homogeneous and isotropic
- Phase change occurs at a discrete temperature and no interfacial/transition/mushy zone is taken into account, essentially meaning interface thickness is zero
- Dendritic growth is not considered yet at the interface
- Conduction is the only mode of heat transfer

3.1.2 Mathematical Framework

Temperature distribution in the solid phase is given as:

$$\frac{\partial^2 T}{\partial x^2} = \frac{1}{\alpha}\frac{\partial T}{\partial t} \qquad T(0,t) = T_0, T(x_f,t) = T_f \qquad k\frac{\partial T}{\partial x}|_{x=x_f} = \rho L\frac{dx_f}{dt} \tag{90}$$

Where k, ρ, α, L are the thermal conductivity, density, thermal diffusivity of the solid phase and latent heat of solidification respectively.

To choose a parameter for the perturbation analysis it should be small enough to serve as the appropriate quantity. The *Stefan Number* is one such quantity under consideration, whose value for some phase change like systems like ice/water have a value less than 0.5 under standard conditions. With this we introduce the following non dimensional quantities

$$\theta = \frac{T - T_f}{T_0 - T_f} \qquad \tau = \frac{kt}{\rho c x_s^2} \qquad \epsilon = \frac{c(T_f - T_0)}{L} \tag{91}$$

Once the above terms have been introduced, to aid in the nondimensionalisation the following quantities have been used to transform (90) into the following equations:

$$\frac{\partial^2 \theta}{\partial x^2} = \frac{\partial \theta}{\partial \tau} \qquad \theta(0,\tau) = 1, \theta(x = x_f, \tau) = 0 \qquad \frac{\partial \theta}{\partial x}|_{x=x_f} = -(1/\epsilon)\frac{dx_f}{d\tau} \tag{92}$$

Perturbation quantity ϵ appears in the boundary condition of the interface in the third condition above. Essentially this condition, also known as the Stefan condition links the transient storage term $\frac{\partial \theta}{\partial \tau}$ with the transient *motion* term $\frac{dx_f}{d\tau}$. Here motion refers to that of the solid liquid interface. Rewriting (92) the following relations can be written

$$\begin{aligned} \frac{\partial \theta}{\partial \tau} = \frac{\partial \theta}{\partial x_f}\frac{\partial x_f}{\partial \tau} \qquad & \frac{\partial \theta}{\partial x}|_{x=x_f} = -(1/\epsilon)\frac{\partial x_f}{\partial \tau} \\ \implies \frac{\partial \theta}{\partial \tau} &= \frac{\partial \theta}{\partial x_f}(-\epsilon\frac{\partial \theta}{\partial x})|_{x=x_f} \\ \implies \frac{\partial^2 \theta}{\partial x^2} &= -\epsilon\frac{\partial \theta}{\partial x_f}(\frac{\partial \theta}{\partial x})|_{x=x_f} \end{aligned}$$

3.1.3 Perturbation Analysis

Now we can derive a perturbation solution by assuming an asymptotic series solution of the form

$$\theta = \sum_{n=0}^{\infty} \theta_n \epsilon^n \tag{93}$$

For ease in analysis we use the first three terms such that

$$\theta = \theta_0 + \epsilon\theta_1 + \epsilon^2\theta_2 \tag{94}$$

Using (94) in the above equations the following modification is made

$$\frac{\partial^2 \theta_0}{\partial x^2} + \epsilon\frac{\partial^2 \theta_1}{\partial x^2} + \epsilon^2\frac{\partial^2 \theta_2}{\partial x^2} = -\epsilon[\frac{\partial \theta_0}{\partial x_f} + \epsilon\frac{\partial \theta_1}{\partial x_f} + \epsilon^2\frac{\partial \theta_2}{\partial x_f}][\frac{\partial \theta_0}{\partial x}|_{x=x_f} + \epsilon\frac{\partial \theta_1}{\partial x}|_{x=x_f} + \epsilon^2\frac{\partial \theta_2}{\partial x}|_{x=x_f}] \tag{95}$$

Using the boundary conditions:

$$\begin{aligned} \theta_0(x = 0, x_f) + \epsilon\theta_1(x = 0, x_f) + \epsilon^2\theta_2(x = 0, x_f) = 1 \\ \theta_0(x = x_f, x_f) + \epsilon\theta_1(x = x_f, x_f) + \epsilon^2\theta_2(x = x_f, x_f) = 1 \end{aligned}$$

Once this is obtained the coefficients of like powers are equated and we obtain

$$\text{Zeroth Order}(\epsilon^0) \qquad \frac{\partial^2\theta_0}{\partial x^2} = 0 \qquad \theta_0(x=0,x_f) = 1, \theta_0(x=x_f,x_f) = 0 \tag{96}$$

$$\text{First Order}(\epsilon^1) \qquad \frac{\partial^2\theta_1}{\partial x^2} = -\frac{\partial\theta_0}{\partial x_f}\frac{\partial\theta_0}{\partial x}|_{x=x_f} \qquad \theta_0(x=0,x_f) = 0, \theta_0(x=x_f,x_f) = 0 \tag{97}$$

$$\text{Second Order}(\epsilon^2) \qquad \frac{\partial^2\theta_1}{\partial x^2} = -[\frac{\partial\theta_0}{\partial x_f}\frac{\partial\theta_1}{\partial x}|_{x=x_f} + \frac{\partial\theta_1}{\partial x_f}\frac{\partial\theta_0}{\partial x}|_{x=x_f}] \qquad \theta_0(x=0,x_f) = 0, \theta_0(x=x_f,x_f) = 0 \tag{98}$$

Historically the zeroth order problem was used by Stefan and physically represents a quasi-steady approximation to the problem. The above equations are solved for calculating the coefficients. The implementation from (96) goes as follows

$$\frac{\partial\theta_0}{\partial x} = C \implies \theta_0 = Cx + D \implies (\text{BC for } \theta_0) \implies \theta_0 = 1 - \frac{x}{x_f}$$

Using the above expression of θ_0 in the higher order expressions

$$\frac{\partial^2\theta_1}{\partial x^2} = -\frac{\partial\theta_0}{\partial x_f}\frac{\partial\theta_0}{\partial x}|_{x=x_f} = \frac{x}{x_f^3}$$

$$\text{Integrating} \qquad \frac{\partial\theta_1}{\partial x} = \frac{x^2}{2x_f^3} + C_1 \implies \theta_1 = \frac{x^3}{6x_f^3} - \frac{x}{6x_f}$$

The expression of θ_2 can be obtained based on the values of θ_1, θ_2 as follows

$$\frac{\partial^2\theta_2}{\partial x^2} = -[\frac{1}{6}(\frac{x}{x_f^3}) + \frac{1}{2}(\frac{x^3}{x_f^5})] \implies \theta_2 = \frac{1}{360}(\frac{x}{x_f})[19 - 10(\frac{x}{x_f})^2 - 9(\frac{x}{x_f})^4]$$

Using the three perturbation terms i.e. $\theta = \theta_0 + \epsilon\theta_1 + \epsilon^2\theta_2$

$$\theta = (1 - \frac{x}{x_f}) - \frac{1}{6}\epsilon(\frac{x}{x_f})(1 - (\frac{x}{x_f})^2) + \frac{1}{360}\epsilon^2(\frac{x}{x_f})(19 - 10(\frac{x}{x_f})^2 - 9(\frac{x}{x_f})^4) \tag{99}$$

Once an expression for θ is obtained the Stefan condition is applied and the following expression is obtained

$$\begin{aligned}\frac{dx_f}{d\tau} &= -\epsilon\frac{\partial\theta}{\partial x}|_{x=x_f} \\ &= \frac{1}{x_f}(\epsilon - \frac{1}{3}\epsilon^2 + \frac{7}{45}\epsilon^3) + O(\epsilon^4)\end{aligned}$$

The final expression for the interface position x_f in terms of the normalised time is given as

$$x_f^2 = (\epsilon - \frac{1}{3}\epsilon^2 + \frac{7}{45}\epsilon^3)2\tau \tag{100}$$

In terms of τ: (mainly used for plotting)

$$\tau = \frac{x_f^2}{2}(\epsilon - \frac{1}{3}\epsilon^2 + \frac{7}{45}\epsilon^3)^{-1}$$

3.1.4 Validation against Similarity solution

In order to validate the results obtained using perturbation analysis, we use the similarity solution approach, discussed in Section II. The problem considered is rewritten as follows (92):

$$\frac{\partial^2\theta}{\partial x^2} = \frac{\partial\theta}{\partial\tau} \qquad \theta(0,\tau) = 1, \theta(x = x_f, \tau) = 0 \qquad \frac{\partial\theta}{\partial x}|_{x=x_f} = -(1/\epsilon)\frac{dx_f}{d\tau}$$

Using similarity technique we have seen a familiar result for θ

$$\theta = 1 - \frac{\text{erf}(\lambda x/x_f)}{\text{erf}\lambda} \qquad \lambda = x_f/2\sqrt{\tau} \tag{101}$$

where λ is the root of the transcendental equation.

$$\sqrt{\pi}\lambda e^{\lambda^2}\text{erf}\lambda = \epsilon \tag{102}$$

One interesting thing to note is that the perturbation solution reproduces **exact** results for *small* values of λ.

In order to do this, a binomial expansion is performed for (102)

$$e^{\lambda^2} = 1 + \lambda^2 + \frac{\lambda^4}{2} + \frac{\lambda^4}{2} + \frac{\lambda^6}{6} + \dots$$
$$\text{erf}\lambda = \frac{2}{\sqrt{\pi}}(\lambda - \frac{\lambda^3}{3} + \frac{\lambda^5}{10} - \frac{\lambda^7}{42} + \dots)$$

Substituting above into (102) the following expression for λ is obtained

$$2\lambda^2 + \frac{4}{3}\lambda^4 + \frac{8}{15}\lambda^6 + \frac{16}{105}\lambda^8 + \dots = \epsilon$$

To obtain a solution for the above λ^2 can be written in terms of a series expansion and reversed, given as $\lambda^2 = \sum_{n=1}^{\infty} b_n\epsilon^n$.

This gives a general expression for λ^2 in terms of ϵ

$$\lambda^2 = \frac{1}{2}\epsilon - \frac{1}{6}\epsilon^2 + \frac{7}{90}\epsilon^3 = \frac{x_f^2}{4\tau} \tag{103}$$
$$x_f^2 = 2\tau(\epsilon - \frac{1}{3}\epsilon^2 + \frac{7}{45}\epsilon^3) \tag{104}$$

3.1.5 Conclusion

In the end we see that the solution for the analytical and perturbation analysis is very similar for small approximation of Stefan Number. We plot some results for ϵ values of $0.2, 0.4, 0.6, 0.8$. From the figure we can comment on a number of things.

- First of all, as the Stefan number increases it takes less time for a certain fixed amount of solidification to take place.
- The difference in solidification curves is more smaller values of Stefan number than for larger values.
- The speed of the interface can be determined from this plot which gives a quantitative understanding about the moving boundary.
- The similarity solution (Section II) gives fairly similar results to the perturbation technique. In order to compare some of these results we use other methods as discussed in the subsequent sections.

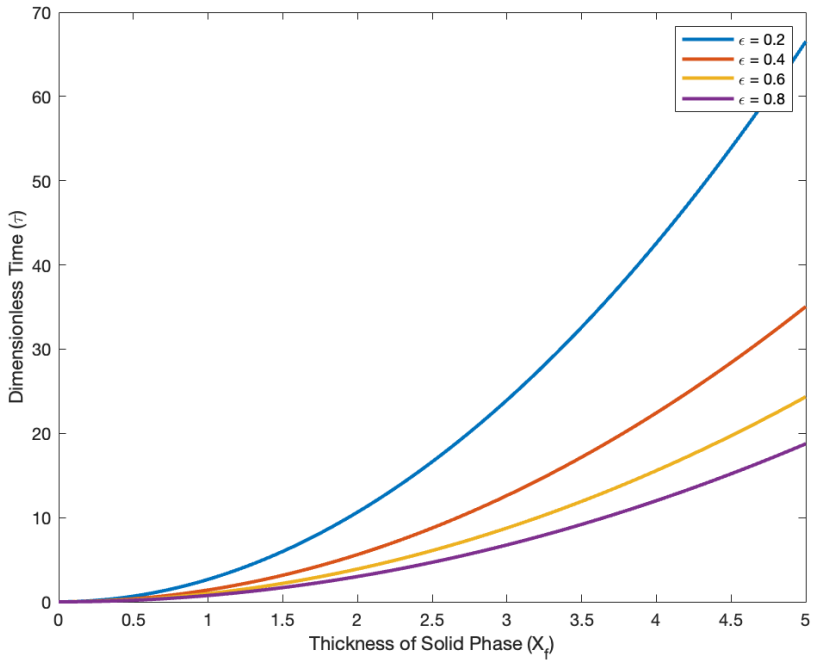

Figure 11: Solidification Thickness vs Dimensionless Time for variable Stefan No. ϵ

4 Analytical Approach III: Multiple Variables Expansion (MVE) Method

Multiple-scale analysis (also known as the method of multiple scales) is a set of techniques used in mathematics and physics to develop consistently valid approximations to the solutions of perturbation problems, for both small and large values of the independent variables. This is accomplished by establishing fast-scale and slow-scale variables for an independent variable, and then treating the fast and slow variables as if they were independent. The ensuing additional flexibility – introduced by the new independent variables – is then employed to remove (unwanted) secular elements during the perturbation problem solution process.

4.1 Solidification with Planar Interface from a Pure Melt

4.1.1 Introduction to Mullins Sekerka Instability

The mathematical analysis of Mullins and Sekerka [26] is aimed at understanding the morphology of the interface; as they themselves explain: *The purpose of this paper is to study the stability of the shape of a phase boundary enclosing a particle whose growth during a phase transformation is regulated by the diffusion of the material or the flow of heat. ... The question of stability is studied by introducing a perturbation in the original shape and determining whether this perturbation will grow or decay.*

In a second seminal paper [27] where they present a rigorous proof for stability of these interfaces they quote: *The purpose of this paper is to develop a rigorous theory of the stability of the planar interface by calculating the time dependence of the amplitude of a sinusoidal perturbation of infinitesimal initial amplitude introduced into the shape of the plane; ... the interface is unstable if any sinusoidal wave grows and is stable if none grow.* With that being the primary motivation in this analysis instability of a planar interface in unidirectional solidification is analysed. The problem considers an originally flat solidifying front advancing into a purely undercooled melt with velocity v.

4.1.2 Basic Framework

A system of moving two dimensional Cartesian coordinate system with the x axis fixed to the interface is considered. The y axis is aligned along the growth direction of the interface. Additionally it is also assumed that mass density ρ, thermal diffusivity constant κ_T, specific heat per unit volume c_ρ are same for both liquid and solid phases. The physical properties are made dimensionless with the governing form expressed as:

$$\lambda\alpha_T(\frac{\partial\bar{T}}{\partial\bar{t}} + \bar{u}\cdot\nabla\bar{T}) = \nabla^2\bar{T} \tag{105}$$

This is the heat conduction equation with the following coordinate transformation in the moving frame. Additionally $\Delta H/(c_p\rho)$ has the scale of temperature and will be used here

$$l_D = \kappa_D/V \qquad \bar{X} = X/l_D \qquad \bar{t} = tV/l_D \qquad \bar{u} = u/V \qquad \bar{T} = \frac{T - T_{MO}}{\Delta H/(c_p\rho)} \tag{106}$$

where T_{MO} refers to melting temperature at the interface. With this we begin the analysis with some boundary conditions. The system under consideration has the form reduced from (105) under the constraints $-|u| = -1, \lambda = 1, \alpha_T = 1$

$$\nabla^2\bar{T} = \frac{\partial\bar{T}}{\partial\bar{t}} - \frac{\partial\bar{T}}{\partial\bar{y}} \tag{107}$$

$$\bar{T} \to T_\infty = \frac{T_\infty - T_{MO}}{\Delta H/(c_p\rho)} \tag{108}$$

The conditions at the interface $\bar{y} = \bar{h}(\bar{x}, \bar{t})$ are

- Thermodynamic equilibrium condition $\bar{T} = \bar{T_S}$
- the Gibbs-Thompson condition: $\bar{T_S} = \gamma \frac{\bar{h}_{\bar{x}\bar{x}}}{(1+\bar{h}_{\bar{x}}^2)^{3/2}}$
- Enthalpy balance equation: $\frac{\partial}{\partial \bar{y}}(\bar{T} - \bar{T_s}) - \bar{h}_{\bar{x}} \frac{\partial}{\partial \bar{x}}(\bar{T} - \bar{T_s}) + \bar{h}_t + 1$

We will skip the bar notation for simplicity in analysis. This one dimensional steady state solution with a flat interface can be obtained by setting the x and t partial derivatives equal to zero. From this we obtain:

$$T_B = e^{-y} - 1 \ \text{(liquid)} \qquad T_B = 0 \ \text{(solid)} \tag{109}$$

where T_B is the basic state solution for temperature. From the expression of liquid temperature it is seen as $y \to \infty \, T_B(\infty) = -1$. Hence the steady state solution is applied only for the general case when $T_\infty = -1$. So the question is what happens when this value is not equal to -1. [28] refers to a situation when $0 > T_B > -1$ and describes the shape of the interface being curved. For cases $T_B < -1$ the system has no solution and it loses thermodynamic equilibrium.

4.1.3 Unsteady Perturbed Solution

To study the pertubation solution for the above problem one chooses primary variables from the steady state solution [28]. These are expressed in the form

$$\begin{aligned} T(x, y, t) &= T_B(y) + \tilde{T}(x, y, t) \\ T_S(x, y, t) &= T_{SB}(y) + \tilde{T_S}(x, y, t) \\ h(x, t) &= h_B + \tilde{h}(x, t) \end{aligned}$$

where $\tilde{T}, \tilde{T_S}, \tilde{h}$ are small perturbations around the steady state.

Accordingly the governing equation for the perturbation is given as

$$\nabla^2 \tilde{T} = \frac{\partial \tilde{T}}{\partial t} - \frac{\partial \tilde{T}}{\partial y} \tag{110}$$

The boundary conditions are as follows:

- As $y \to \infty$, $\tilde{T} \to 0$
- $\tilde{h}$ is very small and the original equations are linearised by expanding them in a Taylor series around $h_B = 0$

The linear interface conditions ar $y = 0$ are written as:

$$\tilde{T} = \tilde{T_S} - (\Delta G_1)\tilde{h} \tag{111}$$

$$\tilde{T_S} = \Gamma \tilde{h_{xx}} - G_{1S}\tilde{h} \tag{112}$$

$$\frac{\partial(\tilde{T} - \tilde{T_S})}{\partial y} + (\Delta G_2)\tilde{h} + \frac{\partial \tilde{h}}{\partial \tilde{t}} = 0 \tag{113}$$

where the G terms imply derivatives given as

$$G_{1L} = \frac{\partial T_B}{\partial \tilde{t}}(0) = -1 \qquad \frac{\partial T_{BS}}{\partial y}(0) = 0 \tag{114}$$

$$\Delta G_1 = (G_{1L} - G_{1S}) = -1 \tag{115}$$

$$\Delta G_2 = \frac{\partial^2 T_B}{\partial y^2}|_{y=0} - \frac{\partial^2 T_{SB}}{\partial y^2}|_{y=0} = 1 \tag{116}$$

Here one additional parameter Γ is introduced which in practice is a small quantity and appears in front of double derivatives. The solution that is sought for in this problem is that of asymptotic expansion solution. In the limiting process when $\Gamma \to 0$ the perturbed quantities have similar order of magnitude which leads to the following relation

$$\epsilon = \sqrt{\Gamma} \tag{117}$$

The parameter ϵ plays a crucial role in the stability of the interface and is hence known as the *interface stability parameter*. The solution sought is predicted to have a nature of multiple length scales [29] and hence attempted to solve using the **Multiple Variables Expansion** method.

In this process one introduces a set of fast variables such that the following relations hold

$$x_+ = \frac{k(\epsilon)x}{\epsilon} \qquad y_+ = \frac{g(\epsilon)y}{\epsilon} \qquad t_+ = \frac{\sigma(\epsilon)t}{\epsilon} \tag{118}$$

Now, the total set of independent variables can be written as $(x_+, y_+, t_+, x, y, \epsilon)$. So now as the interface stability parameter $\epsilon \to 0$ the perturbation solution $\tilde{q} = \tilde{T}, \tilde{T_S}, \tilde{h}$ is expanded as follows

$$\begin{aligned}
\tilde{q}(x_+, y_+, t_+, x, y, \epsilon) \sim e^{t_+}(\tilde{q_0}(x_+, y_+, x, y) + \epsilon\tilde{q_1}(x_+, y_+, x, y) + \dots) \\
k(\epsilon) \sim k_0 + \epsilon k_1 + \dots \\
g(\epsilon) \sim k_0 + \epsilon g_1 + \dots \\
g_s(\epsilon) \sim k_0 + \epsilon g_{s1} + \dots \\
\sigma(\epsilon) \sim \sigma_0 + \epsilon\sigma_1 + \dots
\end{aligned}$$

Notice here that the leading terms of the expansion for $k(\epsilon), g(\epsilon), g_s(\epsilon)$ are set as the same, where k, g, g_s are wave numbers. Using the relations above into (110),(111),(112),(113) and using the following transformation

$$\begin{aligned}
\frac{\partial}{\partial x} &\implies \frac{\partial}{\partial x} + \frac{k}{\epsilon}\frac{\partial}{\partial x_+} \\
\frac{\partial}{\partial y} &\implies \frac{\partial}{\partial y} + \frac{g}{\epsilon}\frac{\partial}{\partial y_+} \\
\frac{\partial}{\partial t} &\implies \frac{\sigma}{\epsilon}\frac{\partial}{\partial t_+} \\
\frac{\partial^2}{\partial x^2} \implies \frac{\partial^2}{\partial x^2} + \frac{2k}{\epsilon}\frac{\partial^2}{\partial x \partial x_+} + \frac{k^2}{\epsilon^2}\frac{\partial^2}{\partial x_+^2}
\end{aligned}$$

The multiple variable form of the final system is thus obtained as:

$$k^2\frac{\partial^2\tilde{T}}{\partial x_+^2} + g^2\frac{\partial^2\tilde{T}}{\partial y_+^2} = \epsilon(\sigma\tilde{T} - g\frac{\partial\tilde{T}}{\partial t_+} - 2k\frac{\partial^2\tilde{T}}{\partial x\partial x_+} - 2g\frac{\partial^2\tilde{T}}{\partial y\partial y_+}) - \epsilon^2(\frac{\partial^2}{\partial x^2} + \frac{\partial^2}{\partial y^2} + \frac{\partial}{\partial y})\tilde{T} \tag{119}$$

$$k^2\frac{\partial^2\tilde{T_S}}{\partial x_+^2} + g^2\frac{\partial^2\tilde{T_S}}{\partial y_+^2} = \epsilon(\sigma\tilde{T_S} - g\frac{\partial\tilde{T_S}}{\partial t_+} - 2k\frac{\partial^2\tilde{T_S}}{\partial x\partial x_+} - 2g\frac{\partial^2\tilde{T_S}}{\partial y\partial y_+}) - \epsilon^2(\frac{\partial^2}{\partial x^2} + \frac{\partial^2}{\partial y^2} + \frac{\partial}{\partial y})\tilde{T_S} \tag{120}$$

Obeying the boundary conditions:

$$\tilde{T} \to 0 \quad (y_+ \to \infty) \qquad \tilde{T_S} \to 0 \quad (y_+ \to -\infty)$$

At the interface the boundary conditions play a crucial role in governing stability. The corresponding equations are:

$$\tilde{T} = \tilde{T_S} - (\Delta G_1)\tilde{h} \tag{121}$$

$$\tilde{T_S} = k^2 \frac{\partial^2 \tilde{h}}{\partial x_+^2} + 2\epsilon k \frac{\partial^2 \tilde{h}}{\partial x_+ \partial x} + \epsilon^2 \frac{\partial^2 \tilde{h}}{\partial x^2} - G_{1S}\tilde{h} \tag{122}$$

$$g\frac{\partial \tilde{T}}{\partial y_+} - g_s \frac{\partial \tilde{T_S}}{\partial y_+} + \epsilon \frac{\partial}{\partial y}(\tilde{T} - \tilde{T_S}) + \sigma\tilde{h} + \epsilon(\nabla G_2)\tilde{h} = 0 \tag{123}$$

As we can see that this closely resembles a system of linear equations, however the linearity comes about in derivatives which needs to be linearised through substitutions.

4.1.4 Zeroth Order Approximation solution

Assuming $\epsilon \ll |k_0| = O(1)$, the zeroth order or leading order approximation can be obtained as

$$k_0^2\left(\frac{\partial^2}{\partial y_+^2} + \frac{\partial^2}{\partial x_+^2}\right)\tilde{T_0} = 0 \tag{124}$$

The boundary conditions take the form:

$$\tilde{T_0} \to 0 \quad (y_+ \to \infty) \qquad \tilde{T_{S0}} \to 0 \quad (y_+ \to -\infty) \tag{125}$$

At the interface the zeroth order terms are:

$$\tilde{T_0} = \tilde{T_{S0}} - (\Delta G_1)\tilde{h_0} \tag{126}$$

$$\tilde{T_{S0}} = k_0^2 \frac{\partial^2 \tilde{h_0}}{\partial x_+^2} - G_{1S}\tilde{h_0} \tag{127}$$

$$k_0 \frac{\partial \tilde{T_0}}{\partial y_+} - k_0 \frac{\partial \tilde{T_{S0}}}{\partial y_+} + \sigma_0 \tilde{h_0} = 0 \tag{128}$$

The zeroth order approximation of the primary variables $\tilde{T_0}, \tilde{T_{S0}}, \tilde{h_0}$ admit mode solutions (essentially exponential solutions so that the system of equations can be linearised).

$$\tilde{T_0} = A_0(x,y)e^{ix_+ - y_+} \qquad \tilde{T_{S0}} = A_{S0}(x,y)e^{ix_+ + y_+} \qquad \tilde{h_0} = \hat{D_0}e^{ix_+} \tag{129}$$

One can replace the exponents $A_0, A_{SO}.$ based on their initial conditions

$$\hat{A_0} = A_0(x,0) \qquad \hat{A_{S0}} = A_{S0}(x,0) \tag{130}$$

Replacing above into (126),(127),(128) we obtain the following

$$\hat{A_0} = \hat{A_{S0}} - \Delta G_1 \hat{D_0} \tag{131}$$

$$\hat{A_{S0}} = -k_0^2 \hat{D_0} - G_{1S}\hat{D_0} \tag{132}$$

$$-k_0(\hat{A_0} + \hat{A_{S0}}) + \sigma_0 \hat{D_0} \tag{133}$$

The linear system of equation just obtained can be solved for a non trivial solution if the determinant of the coefficient matrix is zero. Reframing the coefficient matrix for the above case we have:

$$M = \begin{bmatrix} 1 & -1 & \Delta G_1 \\ 0 & 1 & k_0^2 + G_{1S} \\ -k_0 & -k_0 & \sigma_0 \end{bmatrix}$$

Calculating the determinant of matrix M and using (115) the following relation is obtained

$$\sigma_0 = k_0(1 - 2k_0^2) \tag{134}$$

The above expression is more popularly known as the dispersion relationship. Given the eigenvalue σ_0, the corresponding wavenumber k_0 can be determined.

We also see here that σ_0 must be real. There are few regions to be considered

- When $0 < \sigma < \frac{1}{3}\sqrt{\frac{2}{3}}$, the values of k are $k_0^1 > 0, k_0^2 < 0, k_0^3 > 0$. Negative wavenumber gives unfeasible solution and hence the general solution of the perturbed system is

  $$\bar{h} = Re(D_0^1 e^{ik_0^1 x} + D_0^3 e^{ik_0^3 x}) e^{\frac{\sigma_0}{\epsilon}t}$$

  These solutions are growing unstable modes. In the special case when $\sigma = 0$, $k_0^3 = 0, k_0^1 > 0$ and corresponding solutions are neutrally stable.

- When $\sigma < 0$ the local dispersion relationship yields one real root k_0^1 and one decaying mode

- When $\sigma > \frac{1}{3}\sqrt{\frac{2}{3}}$ the dispersion relationship gives no real root and system has no corresponding mode

Once the fast variable calculations are utilised for the analysis, it is transferred back into the slow variables using the following equations

$$\tilde{T_0} e^{\sigma_0 t_+} = A_0 e^{\tilde{k_0}(ix-y)+\tilde{\sigma_0}t} \tag{135}$$

$$\tilde{T_{S0}} e^{\sigma_0 t_+} = A_{S0} e^{\tilde{k_0}(ix+y)+\tilde{\sigma_0}t} \tag{136}$$

$$\tilde{h_0} e^{\sigma_0 t_+} = D_0 e^{\tilde{k_0}(ix)+\tilde{\sigma_0}t} \tag{137}$$

The dispersion relationship obtained from the non trivial determinant condition is written as:

$$\sigma_0 = k_0(-(G_{1L} + G_{1S}) - 2k_0^2) \implies \tilde{\sigma_0} = \tilde{k_0}(-(G_{1L} + G_{1S}) - 2\epsilon^2 \tilde{k_0}^2) \tag{138}$$

We observe here that G is the temperature gradient. The term $(G_{1L} + G_{1S})/2$ can be viewed as a mean temperature gradient and is condensed as $\bar{G_1}$. Expanding the above equation based on these terms

$$\tilde{\sigma_0} = -2\bar{G_1}\tilde{k_0} - 2\epsilon^2 \tilde{k_0}^3 \tag{139}$$

The above equation (139) is the most fundamental expression to be considered for further analysis. The first term is an unstable factor which is responsible for heat conduction. The second term, known as surface tension, is a stable term but is relevant only when ϵ is large which means for larger length/time scales. These are also called *secular terms*.

For this problem however the surface tension term is eliminated and (139) reduces to

$$\tilde{\sigma_0} = -2\bar{G_1}\tilde{k_0} \tag{140}$$

4.1.5 Analysis of Dispersion Relationship

Since $\bar{G_1}$ is always negative according to the problem (negative mean temperature gradient), one obtains $\tilde{\sigma} > 0$ for $\tilde{k_0} > 0$. Hence this implies that the system will always be unstable.

However one way in which the system can be stable is when the surface tension parameter in (139) is activated and the negative term starts to kick in. However these are short wavelength perturbations and are often dominated by the long wavelength ones which grow in time. Some discussion follows

- For $\tilde{k_0} > \sqrt{\bar{G_1}}/\epsilon, \tilde{\sigma}$ which means the mode solutions are decaying and stable
- For $0 < \tilde{k_0} < \sqrt{\bar{G_1}}/\epsilon$ the mode solutions are growing and unstable.
- For $\tilde{k_0} = \sqrt{\bar{G_1}}/\epsilon$ these are neutral modes with no activity

From this it can be concluded that during solidification every perturbed state is either *purely growing or decaying* owing to Mullins-Sekerka instability. Further when the mean temperature gradient is positive the system is stable for all positive values of $\tilde{k_0}$ as $\tilde{\sigma} < 0$. Physically this means that when the interface moves to a high temperature liquid region the interface will always be smooth. For further analysis however higher order approximations need to be considered specifically for higher length and time scales, i.e when ϵ is taken into account.

5 Analytical Approach IV: Polynomial and Exponential Approximation

5.1 Ice Solidification in a finite domain

The phase change problem of solidification of water in a flat rectangular container, which is a one-dimensional Stephan problem with a moving boundary, is considered. The solution includes determining the moving interface. Stephan problems are parabolic, partial differential heat equations with proper boundary conditions on the moving boundary that are initial boundary value problems. Because of their widespread occurrence in energy conservation units, industrial, refrigeration, crystal growth, geophysical science, welding, and casting, heat transfer problems linked with melting and solidification they have acquired a lot of attention in the last decade. The solidification of pure water in a rectangular capsule is investigated in this study. A constant temperature boundary condition is applied to the enclosure. Conduction is assumed to be the only mode of heat transfer during the solidification process to simplify tracking the interface.

5.1.1 Introduction

The present section discusses an analytical method to evaluate temperature distributions in solid and liquid phase for ice solidification. The process involves considering a polynomial and exponential initial assumption to solve the governing PDE [28]. Finally the results are validated against standard results. The following assumptions are made about the one dimensional problem

- The thermal and physical properties are considered to be constant
- Conduction is the only mode of heat transfer in the medium
- Solid liquid interface boundary moves at a constant rate
- Water temperature in domain is initially at freezing temperature

5.1.2 Mathematical Framework

The solid domain is represented in the domain from $0 < x < y(t)$ and that of liquid as $y(t) < x < h$. T_s and T_l are temperatures of solid and liquid respectively. Interface is denoted by $y(t)$ and a boundary temperature of T_b is imposed. The governing equations for these domains are as follows:

$$k_s \frac{\partial^2 T_s}{\partial x^2} = \rho_s c_s \frac{\partial T_s}{\partial t} \qquad k_l \frac{\partial^2 T_l}{\partial x^2} = \rho_l c_l \frac{\partial T_l}{\partial t} \tag{141}$$

Boundary conditions are given as:

$$T_s = T_b \quad (x = 0) \qquad \frac{\partial T_l}{\partial x} = 0 \quad (x = h) \tag{142}$$

The initial and interface condition is given as

$$T_l(x, 0) = T_m \qquad T_s = T_l = T_m \qquad \rho_s H_s \frac{\partial y}{\partial t} = k_s \frac{\partial T_s}{\partial x} - k_l \frac{\partial T_l}{\partial x} \quad (x = y) \tag{143}$$

The following non dimensional quantities are introduced as follows:

$$\theta = \frac{T - T_b}{T_m - T_b} \qquad X = \frac{x}{h} \quad S = \frac{y}{h} \quad \tau = \frac{k_s t}{\rho_s c_s h^2} \quad \epsilon = \frac{c_s (T_m - T_b)}{H_s} \tag{144}$$

Substituting (144) into (141),(142),(143) we obtain the following dimensionless relations

$$\frac{\partial^2\theta_s}{\partial X^2} = \frac{\partial\theta_s}{\partial\tau} \quad 0 \le X < S \qquad \frac{\partial^2\theta_l}{\partial X^2} = \frac{\alpha_s}{\alpha_l}\frac{\partial\theta_l}{\partial\tau} \quad S < X \le 1 \tag{145}$$

The modified boundary conditions based on the dimensionless transformation changes to

$$\theta_s = 0 \quad (X = 0) \qquad \frac{\partial\theta_l}{\partial X} = 0 \quad (X = 1) \tag{146}$$

Finally the initial and interface conditions changes as:

$$\theta_l = 1 \qquad \theta_s = \theta_l = 1 \qquad \frac{1}{\epsilon}\frac{\partial S}{\partial\tau} = \frac{\partial\theta_s}{\partial X} - \frac{k_l}{k_s}\frac{\partial\theta_l}{\partial X} \quad (X = S) \tag{147}$$

The primary dimensionless equation (145) is then integrated and constraints (146), (147) applied to obtain the following

$$\int_0^S \frac{\partial\theta_s}{\partial\tau}dX = \int_0^S \frac{\partial^2\theta_s}{\partial X^2}dX = \frac{\partial\theta_s}{\partial X}|_S - \frac{\partial\theta_s}{\partial X}|_0 \tag{148}$$

$$\int_S^1 \frac{\alpha_s}{\alpha_l}\frac{\partial\theta_l}{\partial\tau}dX = \int_S^1 \frac{\partial^2\theta_l}{\partial X^2}dX = \frac{\partial\theta_l}{\partial X}|_1 - \frac{\partial\theta_l}{\partial X}|_S \tag{149}$$

Using (148) into (147) we obtain the following

$$\frac{1}{\epsilon}\frac{\partial S}{\partial\tau} = \int_0^S \frac{\partial\theta_s}{\partial\tau}dX + \frac{\partial\theta_s}{\partial X}|_0 + \frac{\rho_l c_l}{\rho_s c_s}\int_S^1 \frac{\partial\theta_l}{\partial\tau}dX \tag{150}$$

Using chain rule $\frac{\partial\theta}{\partial\tau} = \frac{\partial\theta_l}{\partial S}\frac{\partial S}{\partial\tau}$, (150) modifies as

$$\begin{aligned} \frac{1}{\epsilon}\frac{\partial S}{\partial\tau} &= (\int_0^S \frac{\partial\theta_s}{\partial S}dX + \frac{\rho_l c_l}{\rho_s c_s}\int_S^1 \frac{\partial\theta_l}{\partial S}dX)\frac{\partial S}{\partial\tau} + \frac{\partial\theta_s}{\partial X}|_0 \\ \implies \frac{\partial S}{\partial\tau}(\frac{1}{\epsilon} - (\int_0^S \frac{\partial\theta_s}{\partial S}dX - \frac{\rho_l c_l}{\rho_s c_s}\int_S^1 \frac{\partial\theta_l}{\partial S}dX)) &= \frac{\partial\theta_s}{\partial X}|_0 \end{aligned}$$

Now that an equation in θ_s is obtained we use approximations to evaluate the result. As a starting case one uses a linear approximation $\theta_s = a$ to obtain interface velocity as

$$\frac{\partial S}{\partial\tau} = \frac{2\epsilon}{2+\epsilon}\frac{1}{S} \tag{151}$$

5.1.3 Quadratic Approximation

The temperature of the solid region can be assumed to have a quadratic form and expressed as

$$\theta_S = c + dX + eX^2 \tag{152}$$

Applying (146) to the above one obtains

$$dS + eS^2 = 1 \qquad \frac{1}{\epsilon}\frac{\partial S}{\partial\tau} = d + 2eS \implies dS + 2eS^2 = \frac{2}{2+\epsilon} \tag{153}$$

Thus d, e becomes:

$$d = \frac{2(1+\epsilon)}{S(2+\epsilon)} \qquad e = -\frac{\epsilon}{2+\epsilon}\frac{1}{S^2}$$

The expression for solid state temperature is given by

$$\theta_S = \frac{2(1+\epsilon)}{(2+\epsilon)}\frac{X}{S} - \frac{\epsilon}{2+\epsilon}\frac{X^2}{S^2} \tag{154}$$

In order to obtain the interface velocity at this instant we need to calculate $\frac{\partial\theta_S}{\partial X}$, $\frac{\partial\theta_S}{\partial S}$ which gives the interface velocity as:

$$\frac{\partial S}{\partial\tau} = \frac{6\epsilon + 6\epsilon^2}{6 + 6\epsilon + \epsilon^2}\frac{1}{S} \implies S = \frac{1}{2}\sqrt{(\frac{12\epsilon + 12\epsilon^2}{6 + 6\epsilon + \epsilon^2})\tau} \tag{155}$$

5.1.4 Cubic Approximation

As an extension to the earlier model the temperature distribution in the solid region can be approximated by a cubic polynomial given as follows [30]

$$\theta_S = a + bX + cX^3 \tag{156}$$

Using similar boundary conditions as given in (146), one obtains two equations for evaluating the constants namely

$$bS + cS^3 = 1 \qquad bS + 3cS^3 = \frac{2}{2+\epsilon} \implies b = \frac{4+3\epsilon}{2S(2+\epsilon)}, c = -\frac{\epsilon}{2(2+\epsilon)S^3} \tag{157}$$

Substituting back into (156)

$$\theta_S = \frac{4+3\epsilon}{2(2+\epsilon)}\frac{X}{S} - \frac{\epsilon}{2(2+\epsilon)}\frac{X^3}{S^3} \tag{158}$$

Similar to the previous section in order to obtain interface velocity we need to calculate $\frac{\partial \theta_S}{\partial X}, \frac{\partial \theta_S}{\partial S}$ which gives the value as:

$$\frac{\partial S}{\partial \tau} = \frac{4\epsilon}{4+\epsilon}\frac{1}{S} \implies S = \sqrt{\frac{8\epsilon\tau}{4+\epsilon}} \tag{159}$$

5.1.5 Exponential Approximation

While choosing the exponential approximation it can be seen that this ensures an infinite polynomial approximation as compared to the quadratic or cubic ones. The temperature distribution in the solid region is approximated by an exponential function given as

$$\theta_s = a + e^{-bX} \tag{160}$$

Using boundary conditions as in (146), the constants transform to

$$a = -1, b = \frac{-1}{(2+\epsilon)S} \implies \theta_S = -1 + e^{\frac{X}{(2+\epsilon)S}} \tag{161}$$

The following expressions are evaluated

$$\frac{\partial \theta_s}{\partial X}|_0 = \frac{1}{S(2+\epsilon)} \qquad \frac{\partial \theta_s}{\partial S} = e^{\frac{X}{(2+\epsilon)S}}\frac{-1}{(2+\epsilon)}\frac{X}{S^2} \tag{162}$$

which is used to obtain

$$\int_0^S \frac{\partial \theta_s}{\partial S} dX = e^{\frac{1}{(2+\epsilon)}}(1+\epsilon) - (2+\epsilon) \tag{163}$$

from which the interface velocity is easily obtained as:

$$\frac{\partial S}{\partial \tau} = \frac{\epsilon}{(2+\epsilon)(1+\epsilon)((1+\epsilon-\epsilon e^{\frac{1}{(2+\epsilon)}}))}\frac{1}{S} \tag{164}$$

The final expression of S is obtained as

$$S = \frac{1}{2}\sqrt{\frac{2\epsilon\tau}{(2+\epsilon)(1+\epsilon)((1+\epsilon-\epsilon e^{\frac{1}{(2+\epsilon)}}))}} \tag{165}$$

5.1.6 Results and Discussion

From the plots we can see that at a fixed Stefan number the results for Quadratic, Cubic and Exponential are fairly similar. However to verify the results we have used some results from Perturbation Analysis (Section III).

The results show that Cubic analysis gives fairly accurate results with perturbation analysis. This also reflects on the kind of approximation that can be used for a wide range of Stefan values. The error plot of results obtained for a cubic polynomial substitution and perturbative analysis is shown as solidification distance against error which explains the difference. A key observation is that as the Stefan number increases all models correctly predict the increased velocity of the interface as evident from the plots. Finally, during the analysis one **necessarily** needs to choose a linear term while choosing the initial approximation expression. As an exercise one can attempt an analysis *without* the linear term and validate this statement.

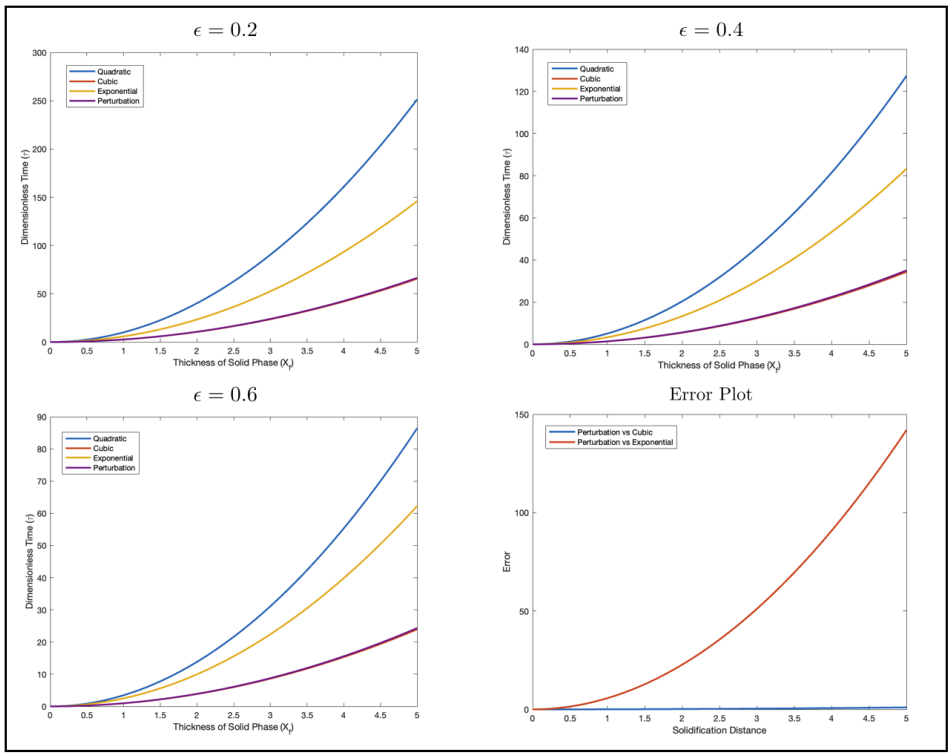

Figure 12: Solidification Distance vs Dimensionless Time for varying Stefan Number (ϵ) and Error Plot for Cubic and Exponential vs Perturbation Analysis

6 Numerical Approach I: Finite Difference Method

6.1 Analysis of Stefan Problem using Finite Difference Method

Finite-difference methods (FDM) are a class of numerical techniques used to solve differential equations by approximating derivatives using finite differences in numerical analysis. The value of the solution at these discrete places is approximated by solving algebraic equations including finite differences and values from neighboring points, and both the spatial domain and time interval (if relevant) are discretized, or broken into a finite number of steps.

Ordinary differential equations (ODE) or partial differential equations (PDE), which may be nonlinear, are converted into a system of linear equations that may be solved using matrix algebra techniques using finite difference methods. The extensive usage of FDM in modern numerical analysis is due to the efficiency with which modern computers can do these linear algebra computations, as well as the relative ease with which they can be implemented. Along with finite element methods, FDMs are one of the most common approaches to the numerical solution of PDEs nowadays.

6.1.1 Introduction

The motivation is driven from the fact that many physical problems involve initial boundary value problems for parabolic differential equations in which part of the boundary is not given a priori but is found as part of the solution. Here we approximate the appearing derivatives of the governing PDE by sums and differences of function values [31]. Two time-stepping schemes used in finite difference for this problem: *Forward Euler* and *Crank Nicholson* [32]. These methods have been discussed in detail and finally implemented.

6.1.2 Forward Euler Method

This method is used for approximating solutions and it is explicit as it can be expressed as the solution at time $n+1$ based on the former step n. To demonstrate and set the framework, the one dimensional heat equation is considered

$$u_t = u_{xx} \qquad x \in (0,1), t \in (0,\infty) \tag{166}$$

$$u(x,0) = v(x) \qquad u(0,t) = u(1,t) = 0 \tag{167}$$

The numerical solution can be written as u_j^n of u as $U_j^n \approx u(jh, nk)$, where $j = 0, 1, 2, \ldots, M, n = 0, 1, 2, \ldots, M$ and $h = 1/M, M$ being the number of nodes in the discretisation and k being the time step. The derivatives are introduced as:

$$\partial_x U_j^n = \frac{U_{j+1}^n - U_j^n}{h} \qquad \bar{\partial}_x U_j^n = \frac{U_j^n - U_{j-1}^n}{h} \tag{168}$$

Using this discretisation, (166) can be written as

$$\partial_t U_j^n = \partial_x \bar{\partial}_x U_j^n \qquad U_0^n = U_M^n = 0 \qquad U_j^0 = v(x_j) \tag{169}$$

Replacing some constants in the problem we take $\lambda = k/h^2$ and rewrite the problem in the following form

$$U_j^{n+1} = \lambda(U_{j-1}^n + U_{j+1}^n) + (1 - 2\lambda)U_j^n \tag{170}$$

$$U_0^{n+1} = U_M^{n+1} = 0 \tag{171}$$

$$U_j^0 = v(x_j) \tag{172}$$

The final form can be expressed in terms of a matrix and that is written as:

$$\bar{U}^{n+1} = A\bar{U}^n \tag{173}$$

where the matrix A is the following

$$A = \begin{bmatrix} 1-2\lambda & \lambda & 0 & \dots & 0 \\ \lambda & 1-2\lambda & \lambda & \dots & 0 \\ 0 & \ddots & \ddots & \ddots & 0 \\ \vdots & \ddots & \lambda & 1-2\lambda & \lambda \\ 0 & \dots & 0 & \lambda & 1-2\lambda \end{bmatrix}$$

As we can see from above the matrix A is a symmetric tridiagonal coefficient matrix.

This method however is only first order accurate in time and second order in space as seen from the above. Hence the error in time dominates unless it is kept too small. Generally speaking the Forward Euler scheme presented above is stable *only* when the mesh ratio, $\lambda \leq 1/2$. This observation is also evident by seeing the diagonal terms in the matrix above and setting the condition that $a_{ii} \geq 0$

6.1.3 Crank Nicholson Scheme

Another finite difference scheme which is a semi implicit one and uses symmetry around a middle point with respect to time $x_j, t_{n+1/2}$

$$t_{n+1/2} = \frac{t^{n+1} + t^n}{k}$$

where k is the time step. Due to the implicit scheme an algebraic system must be solved for in each time step. The same set of equations previously solved by the Forward Euler method can be written as:

$$\bar{\partial}_t U_j^{n+1} = \frac{1}{2}\partial_x \bar{\partial}_x (U_j^n + U_j^{n+1}) \qquad j = 1, 2, \dots, M-1 \tag{174}$$

$$U_0^n = U_M^n = 0 \qquad U_j^0 = v(x_j) \qquad j = 0, 1, \dots, M \tag{175}$$

Arranging the equation in terms of spatial step $n+1$ with n it can be written as

$$(I - \frac{1}{2}k\partial_x\bar{\partial}_x)U_j^{n+1} = (I + \frac{1}{2}k\partial_x\bar{\partial}_x)U_j^n \tag{176}$$

where I is the $M-1$ identity matrix and then using finite difference coefficients to enable writing in the matrix form

$$(1+\lambda)U_j^{n+1} - \frac{1}{2}\lambda(U_{j-1}^{n+1} - U_{j+1}^{n+1}) = (1-\lambda)U_j^n + \frac{1}{2}\lambda(U_{j-1}^n - U_{j+1}^n) \tag{177}$$

The matrix is of the form $B\bar{U}^{n+1} = A\bar{U}^n$ where B can be written as

$$B = \begin{bmatrix} 1+\lambda & -(1/2)\lambda & 0 & \dots & 0 \\ -(1/2)\lambda & 1+\lambda & -(1/2)\lambda & \dots & 0 \\ 0 & \ddots & \ddots & \ddots & 0 \\ \vdots & \ddots & -(1/2)\lambda & 1+\lambda & -(1/2)\lambda \\ 0 & \dots & 0 & -(1/2)\lambda & 1+\lambda \end{bmatrix}$$

and A can be written as

$$A = \begin{bmatrix} 1-\lambda & (1/2)\lambda & 0 & \dots & 0 \\ (1/2)\lambda & 1-\lambda & (1/2)\lambda & \dots & 0 \\ 0 & \ddots & \ddots & \ddots & 0 \\ \vdots & \ddots & (1/2)\lambda & 1-\lambda & (1/2)\lambda \\ 0 & \dots & 0 & (1/2)\lambda & 1-\lambda \end{bmatrix}$$

Since it is a matrix formulation, the resulting solution of field variable can be written as

$$\bar{U}^{n+1} = B^{-1}A\bar{U}^{n} \tag{178}$$

We can see that this problem is second order accurate in time and it no longer enforces restrictions in time step selection.

6.1.4 Transit to the Stefan problem

We introduce some variable transformation in this case owing to the fact that when $t \to 0$ the system turns degenerate.

$$\xi = \frac{x}{s(t)} \qquad u = h(t)F(\xi, t) \tag{179}$$

The PDE transforms as

$$\frac{\partial u}{\partial x} = \frac{\partial^2 u}{\partial x^2} \to h\frac{\partial^2 F}{\partial \xi^2} = s[s\frac{dh}{dt}F + sh\frac{\partial F}{\partial t} - \xi\frac{ds}{dt}\frac{\partial F}{\partial \xi}] \tag{180}$$

For a simple case we assume a non time dependant or constant boundary conditions. How this influences the variables governing the Stefan problem is written as follows.

Let $\beta = \frac{l\rho}{K}$ be a material parameter and the constant boundary conditions imposed on (180) can be written as

$$F = 0 \qquad \xi = 1 \tag{181}$$

$$F = \frac{1}{h(t)} \qquad \xi = 0 \tag{182}$$

$$\beta s(t)\frac{ds}{dt} = -h\frac{\partial F}{\partial \xi} \qquad \xi = 1 \tag{183}$$

The second condition needs some study. The function $h(t)$ must be chosen in such a way that F is independent of time when it tends to 0. The only way that is possible is to choose $h(t) = 1$. The interface evolution equation as obtained from the similarity solution given as $s = 2\Lambda\sqrt{\alpha t}$ can be modified with $\alpha = 1$ changing (180) as:

$$\frac{\partial^2 F}{\partial \xi^2} = -2\Lambda^2\xi\frac{\partial F}{\partial \xi} \qquad F(1) = 0, F(0) = 1, -\frac{\partial F}{\partial \xi}|_{\xi=1} = 2\Lambda^2\beta \tag{184}$$

The final solution is given as

$$F(\xi) = 1 - \frac{\mathrm{erf}(\Lambda\xi)}{\mathrm{erf}(\Lambda)} \tag{185}$$

which satisfies our requirement that $F(\xi, t)$ does not depend on time for the given boundary conditions where Λ has been solved previously in Similarity solution process (Chapter II) and Perturbation analysis (Chapter III).

6.1.5 Numerical solution of Stefan Problem

Given a sufficient background using the numerical scheme discussed so far and boundary conditions applicable for a simplified moving boundary problem the following analysis is performed.

Using (181),(182),(183) and replacing $z = s^2$, (180) transforms as

$$\frac{\partial^2 F}{\partial \xi^2} = z\frac{\partial F}{\partial t} - \frac{\xi}{2}\frac{dz}{dt}\frac{\partial F}{\partial t} \qquad z(0) = 0 \tag{186}$$

The discretisation of the modified problem is carried out using Crank Nicholson scheme which, as discussed, uses a central difference method at time $t^{n+1/2}$ and a second order derivative at ξ_j

$$(1/2)\frac{F_{j+1}^{n+1}-2F_j^{n+1}+F_{j-1}^{n+1}}{h^2}+\frac{F_{j+1}^{n}-2F_j^{n}+F_{j-1}^{n}}{h^2}=$$
$$z^{n+1/2}\frac{F_j^{n+1}-F_j^n}{k}-\frac{\xi_j}{2}\frac{z^{n+1}-z^n}{k}((1/2)\frac{F_{j+1}^{n+1}-F_{j-1}^{n+1}}{2h}+(1/2)\frac{F_{j+1}^{n}-F_{j-1}^{n}}{2h})$$

The boundary conditions transform as:

$$\frac{\beta}{2}(\frac{z^{n+1}-z^n}{k})=-\frac{1}{2}(\frac{F_{M+1}^{n+1}-F_{M-1}^{n+1}}{2h})-\frac{1}{2}(\frac{F_{M+1}^{n}-F_{M-1}^{n}}{2h})\qquad F_0^{n+1}=1,F_M^{n+1}=0 \tag{187}$$

Writing the above in matrix form

$$\tilde{L}=(1/2)\frac{F_{j+1}^{n+1}-2F_j^{n+1}+F_{j-1}^{n+1}}{h^2}-\frac{z^{n+1/2}}{k}F_j^{n+1}+\frac{z'}{8h}\xi_j(F_{j+1}^{n+1}-F_{j-1}^{n+1}) \tag{188}$$

$$\tilde{R}=(-1/2)\frac{F_{j+1}^{n}-2F_j^{n}+F_{j-1}^{n}}{h^2}-\frac{z^{n+1/2}}{k}F_j^{n}+\frac{z'}{8h}\xi_j(F_{j+1}^{n}-F_{j-1}^{n}) \tag{189}$$

This ensured that the left hand side of the equation is structured for $n+1$ step and the right side that of nth step. Some of the notations above are follows:

$$z'=\frac{z^{n+1}-z^n}{k}\qquad z^{n+1/2}=\frac{z^{n+1}+z^n}{2} \tag{190}$$

Including the boundary conditions given in (187) the first step $j=1$ a constant vector is formed given as

$$C=\begin{bmatrix}\frac{1}{h^2}-\frac{z'}{8h}\xi_1\\0\\\vdots\\0\end{bmatrix}$$

Equation (188) can be expanded into a matrix form by assigning

$$A=\frac{F_{j+1}^{n+1}-2F_j^{n+1}+F_{j-1}^{n+1}}{h^2}\qquad B=\frac{z^{n+1/2}}{k}F_j^{n+1}+\frac{z'}{8h}\xi_j(F_{j+1}^{n+1}-F_{j-1}^{n+1})$$

A, B is written as

$$A=\frac{1}{2h^2}\begin{bmatrix}-2&1&0&\dots&0\\1&-2&1&\ddots&\vdots\\0&\ddots&\ddots&\ddots&0\\\vdots&\ddots&1&-2&1\\0&\dots&0&1&-2\end{bmatrix}$$

$$B=\frac{1}{8h}\begin{bmatrix}0&\xi&0&\dots&\dots&0\\\xi_2&0&\xi_2&\ddots&\ddots&\vdots\\0&-\xi_3&0&\xi_3&\dots&0\\0&\ddots&\ddots&\ddots&\ddots&0\\\vdots&\ddots&\ddots&-\xi_{M-2}&0&\xi_{M-2}\\0&\dots&\dots&0&-\xi_{M-1}&0\end{bmatrix}$$

These are examples of tridiagonal matrices. The matrix form can be modified and written as

$$(A-\frac{z^{n+1/2}}{k}I-z'B)F^{n+1}=(-\frac{z^{n+1/2}}{k}I-z'B-A)F^n-2C \tag{191}$$

The above equation can be written as:

$$LF^{n+1} = RF^n - 2C \tag{192}$$

where L and R are the left and right coefficient matrices of (191). In the end including (187) the final form for evaluating z is a second order polynomial equation and expressed as follows

$$\frac{\beta\xi_M}{2k}(z^{n+1})^2 + (-\frac{\beta\xi_M}{k}z^n + \frac{2\beta r}{v} + F_M^{n+1} - F_M^n)z^{n+1} +$$
$$\frac{\beta\xi_M}{2k}(z^n)^2 - \frac{2\beta r}{v}z^n + (2r + z^n)F_M^n - 2r(F_{M-1}^{n+1} + F_{M-1}^n) = 0$$

6.1.6 Results

As we can observe the numerical results agree accurately with the analytical results for small values of Stefan number. The time step t^n is chosen and z is solved which is replaced with $z = s^2$. Interface movement or solidification distance s obtained from the previous step is plotted against time.

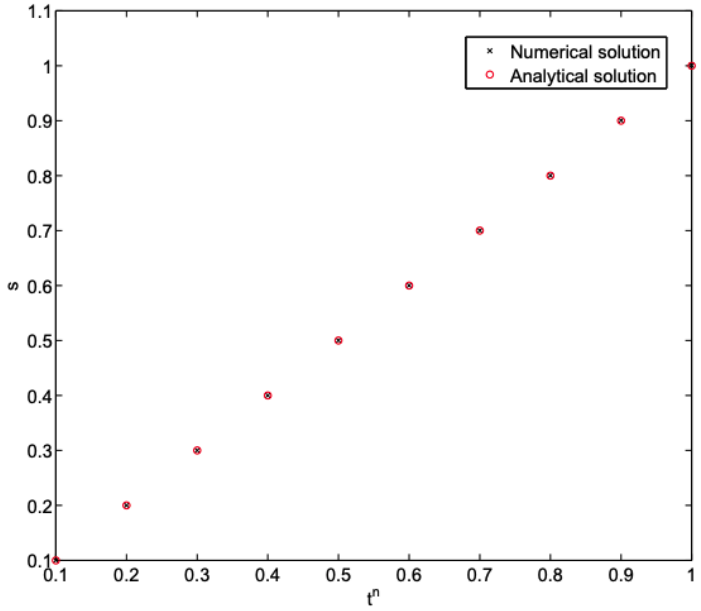

Figure 13: Numerical vs Analytical solution for Time (t^n) against solidification distance (s)

7 Summary

In conclusion we have presented a couple of robust frameworks for solving the one dimensional Stefan problem and observed a number of its quantitative and qualitative aspects. Here is a brief summary of the methods discussed:

- The similarity solution is a fundamental technique for evaluating temperature distributions across a moving boundary. It also gives a transcendental equation for calculating interface position with respect to a given Stefan no vs time. The similarity solution is solved for some example cases and interface attachment kinetics is discussed which find a number of applications today especially in metal additive manufacturing [33].

- The perturbation analysis is discussed after this where a standard approximation is taken for deriving behaviour of the two phase interface during solidification. The results agree with the similarity solution analysis for small values of ϵ and predict boundary movement similar to analytical results. The perturbation method is also used nowadays in the realm of Stefan problem in dendritic growth and anisotropic diffusion [34].

- The Multiple variable expansion analysis is an immensely powerful tool to understand stability of the interface from a geometric and thermodynamic point of view. Using this work the seminal work of Mullins Sekerka is discussed and conditions studied. The analysis is performed for lower order approximations though a higher order one can be used for more accurate results. Despite this, the framework for stability analysis remains the same. One might understand the concept of instability through the various shapes seen in dendritic growth known as Litchenberg figures [35]

- To validate some of the results a simpler technique using cubic and exponential approximation method is used as a starting solution to the field variable. The results are validated against perturbation results which in turn verifies the similarity solution as well. Using this approach the best approximation is estimated and results discussed.

- One numerical method is discussed and presented to gain a quantitative understand of the underlying PDE as well comparing analytical and numerical solution. Two different time stepping schemes are discussed which is Forward Euler and Crank Nicholson. The Stefan problem is numerically evaluated using the Crank Nicholson scheme and results presented. Historically John Crank introduced this method for numerical solution of PDE's specifically for moving boundary problems as discussed in his seminal paper [36].

Other kinds of interfaces such as fluid-fluid can be studied more extensively using numerical tools like Finite Element Analysis and Fourier Spectral methods. These will be addressed in a later communication.

References

[1] Domingo Alberto Tarzia et al. A bibliography on moving-free boundary problems for the heat-diffusion equation. *The Stefan and related problems, MAT-Serie A*, 2, 2000.

[2] RM Furzeland. A comparative study of numerical methods for moving boundary problems. *IMA Journal of Applied Mathematics*, 26(4):411–429, 1980.

[3] Sushil Chandra Gupta. *The classical Stefan problem: basic concepts, modelling and analysis with quasi-analytical solutions and methods*, volume 45. Elsevier, 2017.

[4] Jonathan A Dantzig and Michel Rappaz. *Solidification: -Revised & Expanded*. EPFL press, 2016.

[5] Andrea N Ceretani and Domingo A Tarzia. Similarity solution for a two-phase one-dimensional stefan problem with a convective boundary condition and a mushy zone model. *Computational and Applied Mathematics*, 37(2):2201–2217, 2018.

[6] S Shaw. Perturbation techniques for nonlinear systems. 2001.

[7] Per Jakobsen. Introduction to the method of multiple scales. *arXiv preprint arXiv:1312.3651*, 2013.

[8] Mariela C Olguin, Viviana O Salvadori, Rodolfo H Mascheroni, and Domingo A Tarzia. An analytical solution for the coupled heat and mass transfer during the freezing of high-water content materials. *International Journal of heat and mass transfer*, 51(17-18):4379–4391, 2008.

[9] Miglena N Koleva and Radoslav L Valkov. Numerical solution of one-phase stefan problem for a non-classical heat equation. In *AIP Conference Proceedings*, volume 1293, pages 39–46. American Institute of Physics, 2010.

[10] Nestor Perez et al. *Electrochemistry and corrosion science*, volume 412. Springer, 2004.

[11] K Davey. An analytical solution for the unidirectional solidification problem. *Applied mathematical modelling*, 17(12):658–663, 1993.

[12] Joseph M Savino and Robert Siegel. An analytical solution for solidification of a moving warm liquid onto an isothermal cold wall. *International Journal of Heat and Mass Transfer*, 12(7):803–809, 1969.

[13] Henry Hu and Stavros A Argyropoulos. Mathematical modelling of solidification and melting: a review. *Modelling and Simulation in Materials Science and Engineering*, 4(4):371, 1996.

[14] A Jakhar, P Rath, and SK Mahapatra. A similarity solution for phase change of binary alloy with shrinkage or expansion. *Engineering science and technology, an international journal*, 19(3):1390–1399, 2016.

[15] George W Bluman and Julian D Cole. The general similarity solution of the heat equation. *Journal of Mathematics and Mechanics*, 18(11):1025–1042, 1969.

[16] Vaughan R Voller. A similarity solution for solidification of an under-cooled binary alloy. *International journal of heat and mass transfer*, 49(11-12):1981–1985, 2006.

[17] Herbert E Huppert. The fluid mechanics of solidification. *Journal of Fluid Mechanics*, 212:209–240, 1990.

[18] Pallav Kant, Robin BJ Koldeweij, Kirsten Harth, Michiel AJ van Limbeek, and Detlef Lohse. Fast-freezing kinetics inside a droplet impacting on a cold surface. *Proceedings of the National Academy of Sciences*, 117(6):2788–2794, 2020.

[19] Kimon Symeonidis, Diran Apelian, and M Makhlouf Makhlouf. *The Controlled Diffusion Solidification Process–Fundamentals and Principles*. PhD thesis, Worcester Polytechnic Institute, 2009.

[20] Michael J Aziz. Interface attachment kinetics in alloy solidification. *Metallurgical and materials transactions A*, 27(3):671–686, 1996.

[21] Stephen Danforth Foss. An approximate solution to the moving boundary problem associated with the freezing and melting of lake ice. 1974.

[22] Kenneth G Libbrecht. Snow crystals. *arXiv preprint arXiv:1910.06389*, 2019.

[23] R Trivedi and JT Mason. The effects of interface attachment kinetics on solidification interface morphologies. *Metallurgical Transactions A*, 22(1):235–249, 1991.

[24] Virgil J Lunardini and Abdul Aziz. Perturbation techniques in condition-controlled freeze-thaw heat transfer. Technical report, BATTELLE MEMORIAL INST COLUMBUS OH, 1993.

[25] Raul Ismael Pedroso. *Perturbation techniques for one-dimensional solidification problems*. Columbia University, 1972.

[26] William W Mullins and Robert F Sekerka. Morphological stability of a particle growing by diffusion or heat flow. *Journal of applied physics*, 34(2):323–329, 1963.

[27] William W Mullins and RF Sekerka. Stability of a planar interface during solidification of a dilute binary alloy. *Journal of applied physics*, 35(2):444–451, 1964.

[28] Jian-Jun Xu. Unidirectional solidification and mullins–sekerka instability. In *Interfacial Wave Theory of Pattern Formation in Solidification*, pages 29–74. Springer, 2017.

[29] Jirair K Kevorkian and Julian D Cole. *Multiple scale and singular perturbation methods*, volume 114. Springer Science & Business Media, 2012.

[30] P Bhargavi, Radha Gupta, and Rama Narasimha. Analytical investigation on solidification of ice storage in a rectangular capsule with different temperature profiles. *International Journal of Applied Engineering Research*, 10(20):41424–41430, 2015.

[31] Thomas Clayton Smith. A finite difference method for a stefan problem. *Calcolo*, 18(2):131–154, 1981.

[32] Svetislav Savović and James Caldwell. Finite difference solution of one-dimensional stefan problem with periodic boundary conditions. *International journal of heat and mass transfer*, 46(15):2911–2916, 2003.

[33] HL Wei, T Mukherjee, W Zhang, JS Zuback, GL Knapp, A De, and T DebRoy. Mechanistic models for additive manufacturing of metallic components. *Progress in Materials Science*, 116:100703, 2021.

[34] Martin von Kurnatowski and Klaus Kassner. Selection theory of dendritic growth with anisotropic diffusion. *Advances in Condensed Matter Physics*, 2015, 2015.

[35] Andrew Lindford, Susanna Juteau, Viljar Jaks, Mariliis Klaas, Heli Lagus, Jyrki Vuola, and Esko Kankuri. Case report: Unravelling the mysterious lichtenberg figure skin response in a patient with a high-voltage electrical injury. *Frontiers in Medicine*, 8:861, 2021.

[36] John Crank. Two methods for the numerical solution of moving-boundary problems in diffusion and heat flow. *The Quarterly Journal of Mechanics and Applied Mathematics*, 10(2):220–231, 1957.